Journal of the American Heart Association

ORIGINAL RESEARCH

Human Resistin Induces Cardiac Dysfunction in Pulmonary Hypertension

Qing Lin, MD, PhD; Santosh Kumar, PhD; Udeshika Kariyawasam, PhD; Xiaomei Yang, MD, PhD; Wei Yang, MD, PhD; John T. Skinner, BS; Wei Dong Gao, MD, PhD; Roger A. Johns, MD, PhD

BACKGROUND: Cardiac failure is the primary cause of death in most patients with pulmonary arterial hypertension (PH). As pleiotropic cytokines, human resistin (Hresistin) and its rodent homolog, resistin-like molecule α, are mechanistically critical to pulmonary vascular remodeling in PH. However, it is still unclear whether activation of these resistin-like molecules can directly cause PH-associated cardiac dysfunction and remodeling.

METHODS AND RESULTS: In this study, we detected Hresistin protein in right ventricular (RV) tissue of patients with PH and elevated resistin-like molecule expression in RV tissues of rodents with RV hypertrophy and failure. In a humanized mouse model, cardiac-specific Hresistin overexpression was sufficient to cause cardiac dysfunction and remodeling. Dilated hearts exhibited reduced force development and decreased intracellular Ca^{2+} transients. In the RV tissues overexpressing Hresistin, the impaired contractility was associated with the suppression of protein kinase A and AMP-activated protein kinase. Mechanistically, Hresistin activation triggered the inflammation mediated by signaling of the key damage-associated molecular pattern molecule high-mobility group box 1, and subsequently induced pro-proliferative Ki67 in RV tissues of the transgenic mice. Intriguingly, an anti-Hresistin human antibody that we generated protected the myocardium from hypertrophy and failure in the rodent PH models.

CONCLUSIONS: Our data indicate that Hresistin is expressed in heart tissues and plays a role in the development of RV dysfunction and maladaptive remodeling through its immunoregulatory activities. Targeting this signaling to modulate cardiac inflammation may offer a promising strategy to treat PH-associated RV hypertrophy and failure in humans.

Key Words: cardiac remodeling ■ HMGB1 ■ inflammation ■ RELMα ■ right ventricle

See Editorial by Lemay et al.

Cardiac failure is the primary cause of death in most patients with pulmonary arterial hypertension (PH). As pleiotropic cytokines, human resistin (Hresistin) and its rodent homolog, resistin-like molecule (RELM) α, are mechanistically critical to pulmonary vascular remodeling in PH.[1] However, it is still unclear whether activation of these RELM molecules can directly cause PH-associated cardiac dysfunction and remodeling.

Development of right ventricular (RV) dysfunction (RVD) or RV failure in patients with PH determines their clinical outcome. However, therapies targeting pulmonary vasculature and flow have little success in reducing morbidity and mortality in these patients.[2] Therefore, effective treatment strategies directly targeting RVD are needed. One critical barrier to developing an effective therapy that targets the right ventricle is the poor understanding of the associated pathogenetic mechanisms.

Resistin-like molecules (RELMs) are pleiotropic cytokines with pro-proliferative, pro-inflammatory, profibrotic, vasoconstricting, and chemokine activities. Previous studies point toward their role not only in

Correspondence to: Roger A. Johns, MD, MHS, PhD; Wei Dong Gao, MD, PhD; and Qing Lin, MD, PhD, Department of Anesthesiology and Critical Care Medicine, Johns Hopkins University School of Medicine, 720 Rutland Ave, Baltimore, MD 21205. Email: rajohns@jhmi.edu, wgao3@jhmi.edu, qlin2@jhmi.edu

Supplemental Material is available at https://www.ahajournals.org/doi/suppl/10.1161/JAHA.122.027621

For Sources of Funding and Disclosures, see page 15.

JAHA is available at: www.ahajournals.org/journal/jaha

CLINICAL PERSPECTIVE

What Is New?

- Human resistin (Hresistin) protein is upregulated in right ventricular (RV) tissues of patients with PH, and cardiac-specific Hresistin overexpression in humanized mice causes heart dysfunction and remodeling.
- Hresistin activates damage-associated molecular pattern signaling to trigger cardiac inflammation in RV.
- Anti-Hresistin human antibody ameliorates cardiac hypertrophy and failure in rodent PH models.

What Are the Clinical Implications?

- By using RV tissues from patients with PH, a humanized mouse model of cardiac-specific Hresistin overexpression, and a human antibody targeting Hresistin, we found that Hresistin drives development of RV dysfunction and maladaptive remodeling through its inflammation-promoting activities.
- Our data suggest that Hresistin has a unique role in the immune interaction between lung and RV in humans, mediating remodeling in both organs. Thus, targeting Hresistin signaling may offer a promising strategy to treat PH-associated RV hypertrophy and failure clinically as well as pulmonary vascular remodeling.

Nonstandard Abbreviations and Acronyms

AMPK	AMP-activated protein kinase
DAMP	damage-associated molecular pattern
EP	ethyl pyruvate
HMGB1	high mobility group box 1
Hresistin	human resistin
MHC	myosin heavy chain
NRCM	neonatal rat cardiomyocyte
PH	pulmonary arterial hypertension
PKA	protein kinase A
RELM	resistin-like molecule
RVD	right ventricular dysfunction
SSc	scleroderma
tTA	tetracycline trans-activator

pulmonary vascular remodeling,[3–5] but also in cardiac left ventricle (LV) dysfunction during PH. Systematic injection of experimental rats with an adeno-associated virus with rat resistin gene reportedly induced myocardial dysfunction, especially in the LV.[6]

However, the homolog of rodent resistin could not be identified in humans.[1] Unlike rodent resistin, rodent RELMα and Hresistin are primarily derived from immune cells and have similar inflammation-modulatory functions.[1] Thus, RELMα was recognized as the rodent counterpart of Hresistin.[1] We have shown that rodent RELMα (also known as found in inflammatory zone 1[7] or hypoxia-induced mitogenic factor)[8] and Hresistin have a causal role in PH pathogenesis, because these proteins are mechanistically critical to pulmonary vascular inflammation and remodeling.[3,5,7–17] However, it remained unclear whether RELMα or Hresistin is present in cardiac tissue during PH development and whether activation can directly induce RVD and remodeling.

In the present study, we detected upregulated Hresistin protein in the RV tissue of patients with PH. We also found that RELMα expression was induced in the RV tissue of rodents with cardiac hypertrophy and failure during PH development. In this case, RELMα was present in cardiomyocytes and infiltrating immune cells. To further dissect the cardiac involvement of RELM signaling and more accurately mimic the human disease, we developed the humanized, cardiac-specific, α-myosin heavy chain (MHC)-directed Hresistin knock-in mouse model. We found that Hresistin overexpression in the heart is sufficient to cause cardiac dysfunction and remodeling in mice. These humanized mice had dilated, impaired RVs with decreased intracellular Ca^{2+} availability. Ca^{2+} was associated with the Hresistin regulation of protein kinase A (PKA) and AMP-activated protein kinase (AMPK) in the hearts. Mechanistically, Hresistin overexpression triggered activation of the key damage-associated molecular pattern (DAMP) molecule known as high mobility group box (HMGB)1. The presence of HMGB1 was associated with increased Ki67 proliferation in leukocytes that infiltrated damaged right hearts. Moreover, an antibody that we developed to Hresistin prevented RV hypertrophy in PH and prolonged the survival of experimental rats with failing hearts. Our data indicate that Hresistin plays a direct cardiac role in the pathogenesis of RVD. This knowledge can benefit the search for a new therapeutic approach to PH-accompanied RVD and other related heart diseases in humans.

METHODS

We present a sequence of studies aimed at identifying the role of Hresistin in the pathogenesis of RVD. First we examined stored human cardiac samples of patients with scleroderma (SSc)-associated PH (SSc-PH) and of control patients with non-SSc PH. Next we created and examined induced PH rodent models, both rat and mouse, and compared them with controls. We created a transgenic mouse line to target the mechanistic responses in cardiac tissue. Finally, we

administered anti-Hresistin monoclonal antibodies to rats before induction of PH.

The Johns Hopkins Medicine Institutional Review Board issued type 4 exemption approval before the start of these studies. Animal housing and experimental protocols were approved by the Animal Care and Use Committee of Johns Hopkins University.

The data that support the findings of this study are available from the corresponding author upon reasonable request.

Human Cardiac Tissue

We obtained RV tissue from patients ≥18 years old with SSc-associated PH from stored samples through collaboration with the Johns Hopkins Department of Pathology. For comparison, we also obtained heart tissue from control patients with no signs of PH. These heart samples were collected through biopsy. Clinical data pertaining to these patients with SSc-PH, including right heart catheterization parameters, were published in our previous study.[18]

Generation of a Humanized Transgenic Mouse Model That Overexpresses Hresistin in Cardiomyocytes

We generated a knock-in transgenic MHC-hRETN-overexpressing mouse line that overexpresses cardiac-specific Hresistin. To spatially and temporally control the expression of Hresistin in mouse heart tissue, we generated a dual transgenic inducible overexpression system. Briefly, the model has 2 transgenes. The first contains a promoter-specific sequence encoding a tetracycline trans-activator (tTA). The tTA is a fusion protein made up of a mutated tet Repressor protein and the herpesvirus VP-16 trans-activator,[19] a powerful activator of gene transcription. The tTA protein binds to a tetracycline operator [(otet)7CMV] site, also known as the tetracycline response element, upstream of the Hresistin gene sequence (RETN). The cardiomyocyte-specific MHC promoter was used to drive the expression of the tTA as previously described.[20] The second transgene in these mice contains the RETN gene construct. The construct is composed of (1) a tetracycline response element, (2) a "tight" control sequence to reduce expression of RETN in the absence of tTA, and (3) the RETN cDNA followed by a FLAG tag. The tetracycline response element-Tight-RETN transgene was microinjected into fertilized eggs as described previously.[21] RETN transgene-positive founders were identified and cross-bred with the MHC mice to obtain the double-transgenic mice having cardiac-specific Hresistin overexpression. Trabecular muscles from the RV tissues of MHC-hRETN-overexpressing mice were dissected, and twitch force and intracellular Ca^{2+} concentration ($[Ca^{2+}]i$) were measured as described in our previous studies.[22,23]

Anti-Hresistin Antibody Development and Administration

We used our previously reported techniques to generate anti-Hresistin monoclonal antibodies.[24] They were identified through phage screening of a human library, and screened by ELISA and through plasmon resonance. Potential antibodies were validated for their in vitro antiproliferative function against Hresistin in human primary pulmonary smooth muscle cells. They were further screened for immunogenicity, manufacturability, and toxicity.[24] The human antibodies exhibited cross reactivity to block rodent RELMα in smooth muscle cell assays.[24] For therapeutic antibody administration in this study, rats received twice weekly intraperitoneal injections of 4 mg/kg before we began induction of PH by hypoxia or monocrotaline.

Animal Models of PH

Our PH rodent models were induced by monocrotaline[22,25] or hypoxia[10] as we have described previously. Animals were maintained at 20 to 24 °C with a 12:12-hour light–dark cycle with access to normal laboratory diet (Teklad global 18% protein rodent diet; Envigo) and chlorinated water ad libitum. Cage bedding was also from Envigo (7097 Teklad corncob bedding).[16] For induction of the hypoxia-induced PH model, 8- to 12-week-old male C57BL/6 mice or 250 to 300 g male Sprague–Dawley rats (Charles River Laboratories, Wilmington, MA) were exposed to 10.0% O_2 (hypoxia) for 4 or 28 days and then euthanized and processed as described previously.[10] Control mice were exposed to normal room air (20.8% O_2, normoxia). As we have explained previously,[16] given the reports that estrogens exhibit protective effects in classical rodent PH models,[26,27] and the finding that the damage-associated inflammatory response is more profound in male rodents with PH than in corresponding female rodents,[28] we used only male rodents to produce a more severe disease and investigate the Hresistin-regulated DAMP signaling.[16] Each animal was identified using a numbered ear tag. Investigators performing procedures on the animals were blinded to the group assignment. Animals in each group were unblinded once data analysis was completed. The group sizes were determined by power calculations. We ensured that experiments were unbiased by following the recent guidelines for PH preclinical and translational research.[29,30] For the monocrotaline-induced RVD model, 250 to 300 g male Sprague–Dawley rats from Charles River were randomized to subcutaneous injection with monocrotaline 60 mg/kg (Sigma Aldrich) or vehicle control. For

the echocardiographic analysis, before anesthesia for hemodynamic and other analyses, each rat underwent transthoracic echocardiography in an awake state on the indicated time points. The hearts were harvested at the following time points: (1) control, no intervention; (2) RV hypertrophy, defined as compensated hypertrophic RV (significantly increased RV wall thickness and RV size, as compared with the nonmonocrotaline control) with maintained contractility (as indicated by the RV ejection fraction) (2.5–4.0 weeks postmonocrotaline injection)[22]; (3) RV failure, defined as decompensated (hypertrophic) RV with significantly decreased contractility (4.5 weeks postmonocrotaline injection); in this decompensated stage, the rats clinically exhibited signs of RV failure including low food intake, retarded weight gain, and lack of daily activity.[25] Between 5 and 6 weeks after monocrotaline treatment, the key hemodynamic index cardiac output, calculated by echocardiography, was >70% decreased.[22,25] This is comparable to the cardiac output values calculated by catheterization (≈50% decrease) in the same decompensated stage and the same monocrotaline rat model by other groups.[31–33] The rats entering the decompensating phase exhibited increased morbidity and mortality. Their survival curves were recorded.

RV Systolic Pressure and Fulton Index

For measurement of RV systolic pressure, the hypoxia-treated (or control normoxia) rats were weighed, and sustained anesthesia was induced by intraperitoneal injections of ketamine (100 mg/kg) and xylazine (10 mg/kg). A trachea cannula was inserted, and the animal was ventilated with a Harvard Rodent Ventilator Model 683 (1.2–2.5 mL/breath and 70–81 breaths/min); rocuronium was injected intraperitoneally (2 mg/kg) as a paralytic. Rat body temperature was monitored and controlled via rectal probe connected to a TCAT 2LV Controller (Physitemp, Clifton, NJ) to provide continuous feedback. The chest was opened to expose the heart. RV systolic pressure was measured via apical stab followed by insertion of a 1.4F pressure-volume catheter (SPR-839, Millar Instruments, Houston, TX) into the right ventricle. Data were collected with the AD Instruments Powerlab 8/35 (AD Instruments, Colorado Springs, CO) and Millar MPVS Ultra. Rats were allowed to reach a stable baseline (≈10–15 minutes) before we recorded 3 nonventilated pressures to determine mean RV systolic pressure per animal. After hemodynamic measurements, rats were euthanized by exsanguination, and the heart was removed en bloc and bisected into the RV and LV plus septum. Each portion of the heart was weighed, and the RV and LV plus septum ratio was determined as the Fulton index. For the echocardiographic analysis of these rats exposed to hypoxia or control normoxia, before anesthesia for hemodynamic and other analyses, each rat underwent transthoracic echocardiography in an awake state. Here we report M-mode evaluation of RV thickness and pulmonary artery Doppler flow analysis of pulmonary acceleration time/pulmonary ejection time ratio.

Immunoprecipitation

We assessed binding of the human therapeutic antibody against Hresistin to rodent RELMα by immunoprecipitation. We incubated 2 μg of the anti-Hresistin antibody with 100 ng of laboratory-made FLAG-tagged recombinant rat RELMα protein and Dynabeads Protein A (10001D, Thermo Fisher, Waltham, MA). Protein–antibody binding was detected by western blotting with anti-Hresistin antibody (AF1359, R&D Systems, Minneapolis, MN). Recombinant rat RELMα protein (30 ng) served as a positive loading control.

Trabecular Muscles

Twitch force and intracellular Ca^{2+} concentration ($[Ca^{2+}]i$) were measured as described in our previous studies.[20,24] Trabecular muscles from the right ventricle were dissected, mounted between a force transducer and a motor arm, superfused with Krebs–Henseleit solution at a rate of ≈10 mL/min, and stimulated at 0.5 Hz. The dissecting Krebs–Henseleit solution was composed of (in mmol/L) NaCl 120, $NaHCO_3$ 20, KCl 5, MgCl 1.2, glucose 10, $CaCl_2$ 0.5, and 2,3-butanedione monoxime 20 (pH 7.35–7.45 at room temperature [21–22 °C]). Force was measured by a force transducer and $[Ca^{2+}]i$ was measured by using fura-2. The muscles underwent isometric contractions with the resting muscle length set such that resting force was 15% of total force development (optimal muscle length).

In Vitro Culture, Treatments, and Assessment of the Cardiomyocytes Isolated From Neonatal Rats

Neonatal rat cardiomyocytes (NRCMs) were isolated from 1- to 3-day-old Sprague–Dawley pups and cultured in DMEM as we previously described.[34] NRCMs were serum starved in DMEM containing 0.1% insulin transferrin selenium (Thermo Fisher) for 24 hours and then incubated with the anti-Hresistin antibody at 3 μg/mL (a dose that has blocking activities against Hresistin recombinant protein without cytotoxic effects[24]) or with 5 μmol/L HMGB1 inhibitor ethyl pyruvate (EP) (#E47808, Sigma). After stimulation, NRCMs were transfected with MOI-300 green fluorescent protein–tagged adeno-associated virus expressing the Hresistin (*hRETN*) (the viral vectors containing the ubiquitous CB promoter were produced by the University of Florida Vector Core Laboratory, as we previously

described[3,9]). After 24 hours, some treated/transfected NRCMs were harvested for western blotting analysis. For the cell surface area measurement, after treatment and transfection of the cultured NRCMs, real-time live cell images were captured using the IncuCyte S3 Live-Cell Analysis System and analyzed using the IncuCyte software to calculate cardiomyocyte area, as we previously described.[34]

Quantitative Real-Time Polymerase Chain Reaction

Total RNA was isolated with the RNeasy kit (Qiagen) according to the manufacturer's protocol. Total RNA (500 ng) was reverse transcribed into cDNA. Quantitative polymerase chain reaction was carried out on an ABI 7500 fast real-time polymerase chain reaction system (Applied Biosystems, Foster City, CA). Fold changes in gene expression were acquired by using the delta method and normalization to 18 S rRNA. The primers used in this process were 5′-CAATCCCATGGCGTATA AAAGCATC-3′ (RELMα forward), 5′-TCATTCTTAGG ACAGTTGGCAGCAG-3′ (RELMα reverse), 5′-TGAGC AAGAGAGGCCCTATC-3′ (GAPDH forward), and 5′-AGGCCCCTCCTGTTATTATG-3′ (GAPDH reverse).

Immunohistology

We used immunofluorescence staining to detect the expression of FLAG-tagged Hresistin in the RV tissue of knock-in mice. After deparaffinization of tissue, rehydration, and antigen retrieval, sections were treated with anti-heavy chain cardiac myosin (ab185967, Abcam) and anti-FLAG (F1804, Sigma) antibodies overnight at 4 °C and then with Alexa Fluor488-donkey anti-mouse IgG (715–545-150, Jackson ImmunoResearch) and Cy3-donkey anti-rabbit IgG (711–166-152, Jackson ImmunoResearch) for double fluorescence staining. In the monocrotaline model, rat RV sections were treated with anti-RELMα (AF1523, R&D Systems) and anti-myosin (ab185967, Abcam) antibodies, whereas human RV tissue from SSc-PH patients were treated with anti-Hresistin antibody (AF1359, R&D Systems) for immune staining. In other Immunofluorescent studies, RV tissue from monocrotaline-treated wild-type rats, hypoxic wild-type mice, and MHC-hRETN mice were sliced and stained with anti-Ki67 (ab16667, Abcam) or anti-HMGB1 (ab18256, Abcam) antibodies, with or without co-staining of anti-heavy chain cardiac myosin (ab185967, Abcam), F4/80 (ab6640, Abcam), myeloperoxidase (MPO; AF3667, R&D), or vimentin (ab8978, Abcam). Sections were then incubated with the appropriate fluorochrome-coupled secondary antibody (Jackson ImmunoResearch). Finally, all sections were mounted in ProLong Gold anti-fade reagent with DAPI (Invitrogen). Staining was imaged and tissue sections were analyzed by confocal microscopy (Leica SPE DMI8).

Western Blotting

The collected mouse/rat heart tissues or NRCMs in RIPA buffer (Sigma) (supplemented with 1 mmol/L phenylmethylsulfonyl fluoride, 1 mmol/L Na_4VO_3, and protease inhibitor mixture [Roche, 116974980011]) were lysed with homogenization beads (0.9–2.0 mm; SSB14B, Bullet Blender) in a Bullet Blender at 4 °C, vortexed, and then centrifuged. The concentration of isolated proteins was measured by the bicinchoninic acid method (BCA kit, Bio-Rad). The supernatants were mixed in SDS sample loading buffer (NuPAGE, Invitrogen) at 99 °C for 10 minutes and then subjected to SDS-PAGE. After electrophoresis, proteins were transferred onto polyvinylidene difluoride membranes and immunoblotted with antibodies to RELMα (AF1523, R&D Systems), total PKA C (4782, Cell Signaling), phospho-PKA C (5661, Cell Signaling), total AMPK (Ab131512, Abcam), phospho-AMPK (50 081, Cell Signaling), HMGB1 (ab18256, Abcam), Ki67 (ab16667, Abcam), or GAPDH (G8795, Sigma) overnight at 4 °C, and then probed with horseradish peroxidase–conjugated secondary antibodies (Bio-Rad) for 2 hours. Protein bands were visualized by chemiluminescence (ECL; Amersham Pharmacia Biotech, Arlington Heights, IL).

Statistical Analysis

Data are presented as the mean±SEM. Comparisons between 2 groups were analyzed by Student *t* test, and comparisons of multiple groups were analyzed by 1-way ANOVA followed by the Newman–Keuls post hoc test unless otherwise noted: the Tukey post hoc test was used for the immunoblotting analysis in the RV of antibody-treated rats, and the log-rank test was used for the survival analysis. All statistical analyses were performed with Prism 7.0 e (GraphPad Software, La Jolla, CA). A $P < 0.05$ was considered statistically significant.

RESULTS

We found evidence to suggest that RELMα/Hresistin signaling contributes to RVD in parallel with PH development in rodents as well as humans. In addition, Hresistin knock-in mice displayed RVD, as seen in RV remodeling, impaired contractility, and induced myocyte hypertrophy and fibrosis. We also examined evidence of HMBG1 signaling in monocrotaline-induced rats and Hresistin knock-in mice, identifying a pathological temporal progression in rats. In addition, administration of the antagonist EP inhibited HMGB1 release

in rats. Finally, we administered an anti-Hresistin human antibody in the chronic hypoxia-induced PH rat model with promising results for therapeutic application.

Hresistin/RELMα Expression in RV Tissues of PH Rodent Models and Patients

Before examining the expression of Hresistin/RELMα, the monocrotaline-treated rats were tested by echocardiography (Figure S1A) and categorized as normal (RV wall thickness: 0.49 ±0.01 mm; RV chamber diameter: 2.46±0.08 mm; ejection fraction: 70.6±6.4%), RV hypertrophy (RV wall thickness: 0.59±0.02 mm; RV chamber diameter: 2.82±0.20 mm; ejection fraction: 75.2±2.1%), and RV failure (RV wall thickness: 0.60±0.02 mm; RV chamber diameter: 3.22±0.10 mm; ejection fraction: 61.9±3.5%). These echocardiography data were consistent with that of our previous studies on the monocrotaline rat model.[22,25] We also characterized the experimental rats at the histologic level with Masson's trichrome analysis (Figure S1B), which showed that monocrotaline drove progressive and severe RV fibrotic remodeling. Following the study on the RV status, we found that the rodent homolog of Hresistin was upregulated in the RV tissues of the

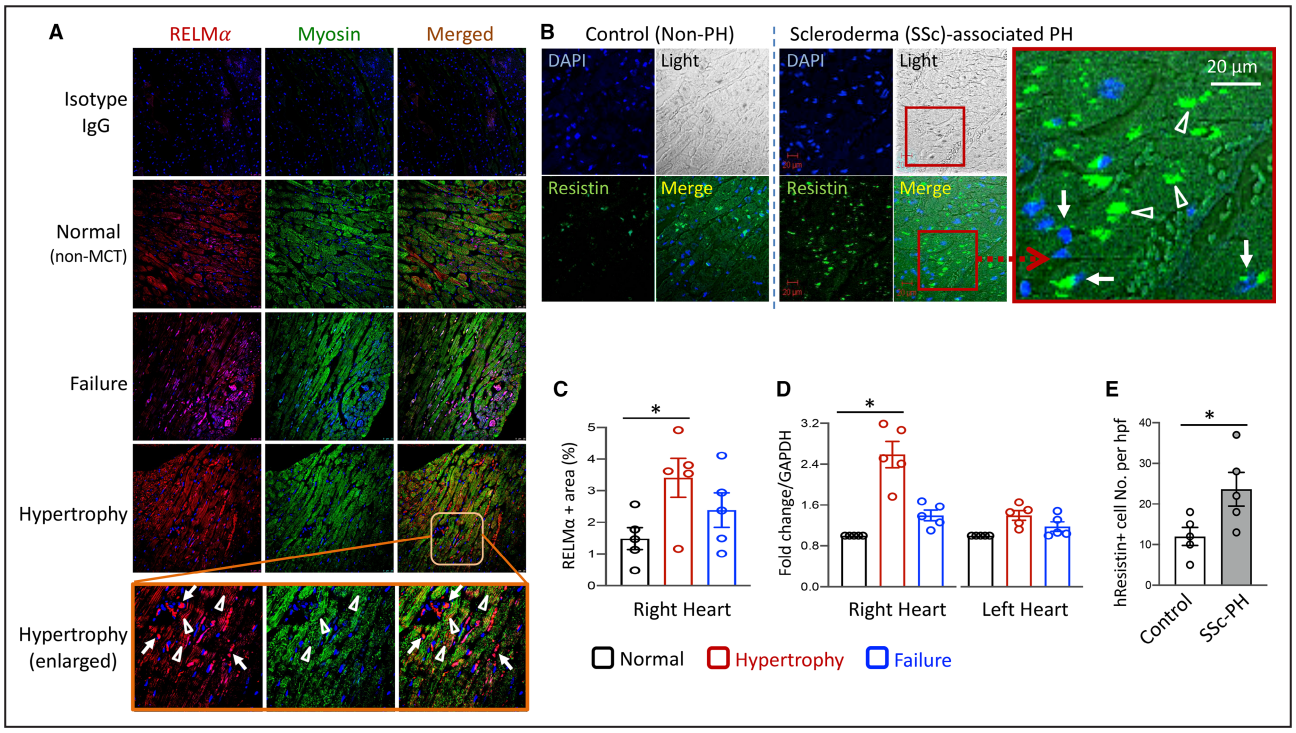

Figure 1. Expression of Hresistin/RELMα during right ventricular dysfunction.
A, Immunofluorescence images of RV tissue slices from monocrotaline (MCT)-treated rats and normal controls. Sections were stained with anti-RELMα (red), co-stained with anti-myosin (green), and counterstained with DAPI. Original magnification: ×200. The bottom panels show the outlined area from the 2-week post-MCT time point at higher magnification (×400). The arrowheads point to the myosin (green)-labeled cardiomyocytes positively stained for RELMα (red), whereas the arrows point to the myosin-negative RELMα-positive immune cells that infiltrated into the myocardial interstitium. Representative images are from 5 individual RV samples per group. **B**, Hresistin detection in human RV tissue (n=5 subjects per group). Confocal images show Hresistin (green signal) staining in the RV heart biopsy of non-PH control subjects and patients with scleroderma (SSc)-associated pulmonary arterial hypertension. Light micrograph of fluorescence images to show structure. Signals of light micrograph (showing tissue structure) and fluorescence images (of Hresistin and DAPI staining) are digitally merged and the boxed area is enlarged and displayed in the right panel. The arrowheads point to the Hresistin protein signals in cardiomyocytes whereas the arrows point to the Hresistin-positive staining in the infiltrating immune cell. **C**, Quantitative analysis of data in (**A**). Percentage of areas positive for RELMα in rat RV tissues was determined by the histogram tool with Adobe Photoshop software. Data are presented as mean±SEM (n=5 animals per group). *P<0.05 vs normal group. **D**, Quantitative real-time PCR analysis of RELMα genes in the right heart and left heart tissues of MCT-injected rats (n=5 animals per group; the dots in the graphs represent single individuals) with cardiac hypertrophy (2 weeks post-MCT) and failure (4 weeks post-MCT). **E**, Quantitative analysis of data in (**B**). The Hresistin-positive (+) cells were counted and expressed as numbers per high-power field (hpf). Data are presented as mean±SEM (n=5 subjects per group). *P<0.05. DAPI indicates 4'6-diamidino-2-phenyl-indole; Hresistin, human resistin; PCR, polymerase chain reaction; PH, pulmonary arterial hypertension; RELMα, resistin-like molecule-α; and RV, right ventricular.

monocrotaline-induced PH model. Protein (Figure 1A and 1C) and gene (Figure 1D) expression of RELMα in rats was especially clear in the hypertrophic remodeling RV, as compared with that in the RV of control rats or in the unaffected LV of the same heart. Furthermore, costaining revealed that endogenous RELMα was localized to both infiltrating immune cells and cardiomyocytes of rats with RVD and right ventricular failure (Figure 1A), indicating cellular sources of this cytokine. Of note, in cardiac biopsy samples from patients with SSc-PH, immunofluorescence analysis also detected the upregulated Hresistin protein signal in RV tissues of patients with PH compared with those of non-PH control subjects (Figure 1B and 1E). The expression of Hresistin was observed in the immune cells and cardiomyocytes of patients with PH (Figure 1B), consistent with that of RELMα in PH rats (Figure 1A). These data indicate that RELMα/Hresistin signaling in the RV contributes to RVD development in parallel with pulmonary vascular remodeling in lungs during PH development.[16,17]

Cardiac-Restricted Hresistin Overexpression Causes Cardiac Dysfunction and Remodeling

The Hresistin knock-in mice were generated through a direct cardiac overexpression (cross with MHC promoter) of recombinant Hresistin (Figure 2A and 2B). We validated Hresistin protein (Figure 2C) and gene (Figure 2D) expression in the RV tissues of these cardiac-specific Hresistin humanized mice. Functional assessment of trabecular muscle samples isolated from the MHC-Hresistin-overexpressing RVs revealed decreased twitch force and intracellular Ca^{2+} transients (Figure 3A). This indicates depression of excitation–contraction coupling. We then tested key calcium-modulating protein kinases and found that phosphorylation of both PKA (Figure 3B) and AMPK (Figure 3C) were mitigated in the Hresistin-overexpressing cardiac tissues. In isolated myocytes, wheat germ agglutinin cell boundary staining revealed that Hresistin-overexpressing myocytes were larger than control myocytes (Figure 3D). Moreover, hearts that overexpressed Hresistin exhibited increased fibrosis, another key feature of remodeling (Figure 3E). These results indicate that cardiac Hresistin overexpression

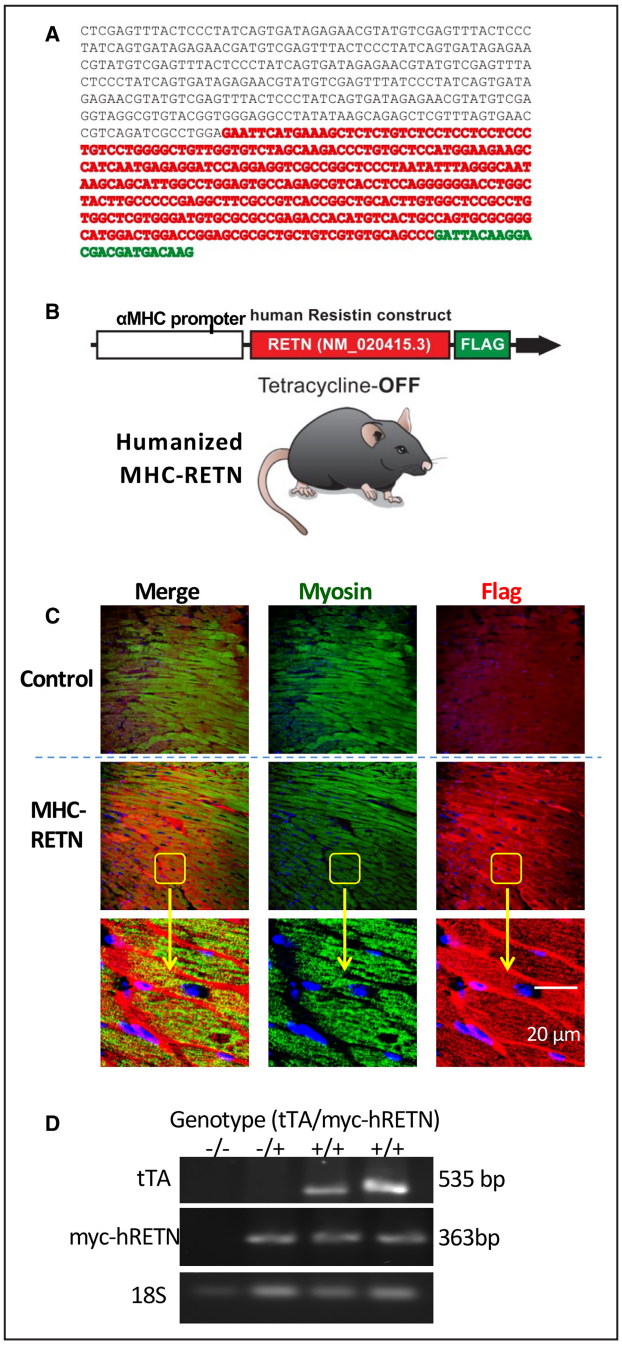

Figure 2. Generation of cardiac-specific Hresistin transgenic mice.

A and **B**, Images present the nucleotide sequence for the Hresistin (hRETN) construct (**A**) and a schematic representation of the αMHC-hRETN transgene structure (**B**). **C**, Immunofluorescence images of heart tissue samples from hRETN cardiac-overexpressing humanized mice and their corresponding littermate controls. Sections were stained with anti-myosin (green), co-stained with anti-FLAG (red), and counterstained with DAPI to validate the expression of the FLAG-tagged hRETN protein. Separate channels are displayed in middle and right panels, and digitally merged in left panels. Original magnification: ×200. Boxed areas are shown at higher magnification (×400) in the lower panels. Images are representative of 3 individual heart samples. **D**, Genotyping by PCR analysis of genomic DNA. Amplification of a 363-bp product encoding the myc-RETN epitope region of the transgene indicates that the humanized animals carry the knock-in hRETN gene in hearts. A 535-bp product was specifically amplified from animals carrying the tTA transgene. The 494-bp 18S housekeeping gene served as a control. DAPI indicates 4'6-diamidino-2-phenyl-indole; MHC, myosin heavy chain; PCR, polymerase chain reaction; and tTA, tetracycline trans-activator.

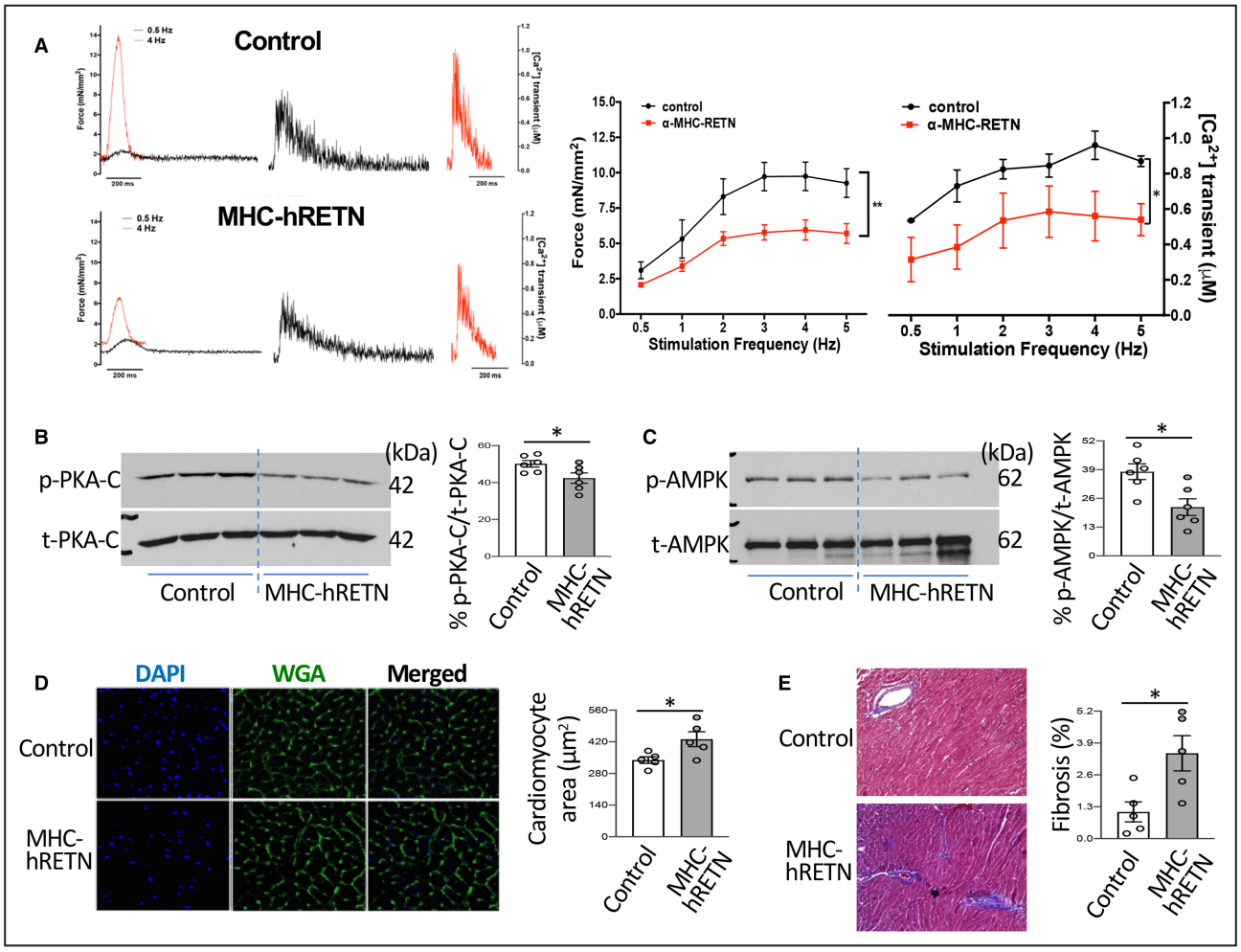

Figure 3. Cardiac dysfunction and remodeling in humanized mice that overexpress MHC-hRETN.
A, Pooled data of force-frequency (left panel) and intracellular Ca^{2+} transient-frequency (right panel) relationships in trabecular muscles from RV of wild-type and cardiac-specific MHC-hRETN-overexpressing mice (in force-frequency test: n=6 and 5 for control and overexpressing mice, respectively; in Ca^{2+} transient-frequency test: n=4 animals per group; the 2 assays used samples from different animals). **P*<0.05, ***P*<0.01. **B** and **C**, Changes in phosphorylation of PKA (B) and AMPK (C) in cardiac tissue from cardiac-specific MHC-hRETN-overexpressing mice and control littermates were determined by western blotting. Left panels show representative immunoblots. Right panels show quantitative analysis of expression. Data are shown as mean±SEM (n = 6 animals per group). **P*<0.05 vs control littermates. *P*- indicates phosphorylated protein; t- indicates total protein. **D**, Wheat germ agglutinin (WGA) cell boundary staining in the Hresistin-overexpressing myocytes. Left panels: heart tissue samples show cell nuclei (blue) and cell boundary (green). Magnification: ×400. Right panels: quantification of cell surface area based on histologic analysis of cardiomyocytes. Data represent means±SEM (n=5 animals per group). **P*<0.05 vs littermate control group. **E**, Masson's trichrome staining of heart tissue samples from MHC-Hresistin (RETN) humanized and littermate control groups. Magnification: ×200. Representative images (left panels) and quantitative analysis (right panels) were presented. Pooled data for quantification of fibrosis from 5 randomly selected histological fields at a magnification of ×400 on each slide. Data are shown as mean±SEM (n=5 animals per group). **P*<0.05 vs control group. AMPK indicates AMPK-activated protein kinase; DAPI, 4'6-diamidino-2-phenyl-indole; hRETN, human resistin; MHC, myosin heavy chain; and PKA, protein kinase A.

impairs cell function and induces myocyte hypertrophy and fibrosis.

Hresistin Triggers DAMP-Dependent Inflammatory Signaling in RV

The Hresistin-inhibited AMPK phosphorylation (Figure 3C) suggested the DAMP pathway. As in a rodent lipopolysaccharide-induced acute lung injury model, Hresistin-induced AMPK attenuation was linked to the activation of the alarmin HMGB1.[35] We also identified Hresistin/RELMα as an upstream regulator of HMGB1 in the hypoxic lung.[16,17] We explored the proinflammatory pathways triggered by Hresistin by examining HMGB1 signaling and observed high numbers of HMGB1-expressing cells in the hypertrophic and failing RV tissue of monocrotaline-treated rats (Figure 4A through 4C). Interestingly, a substantial number of HMGB1-positive,

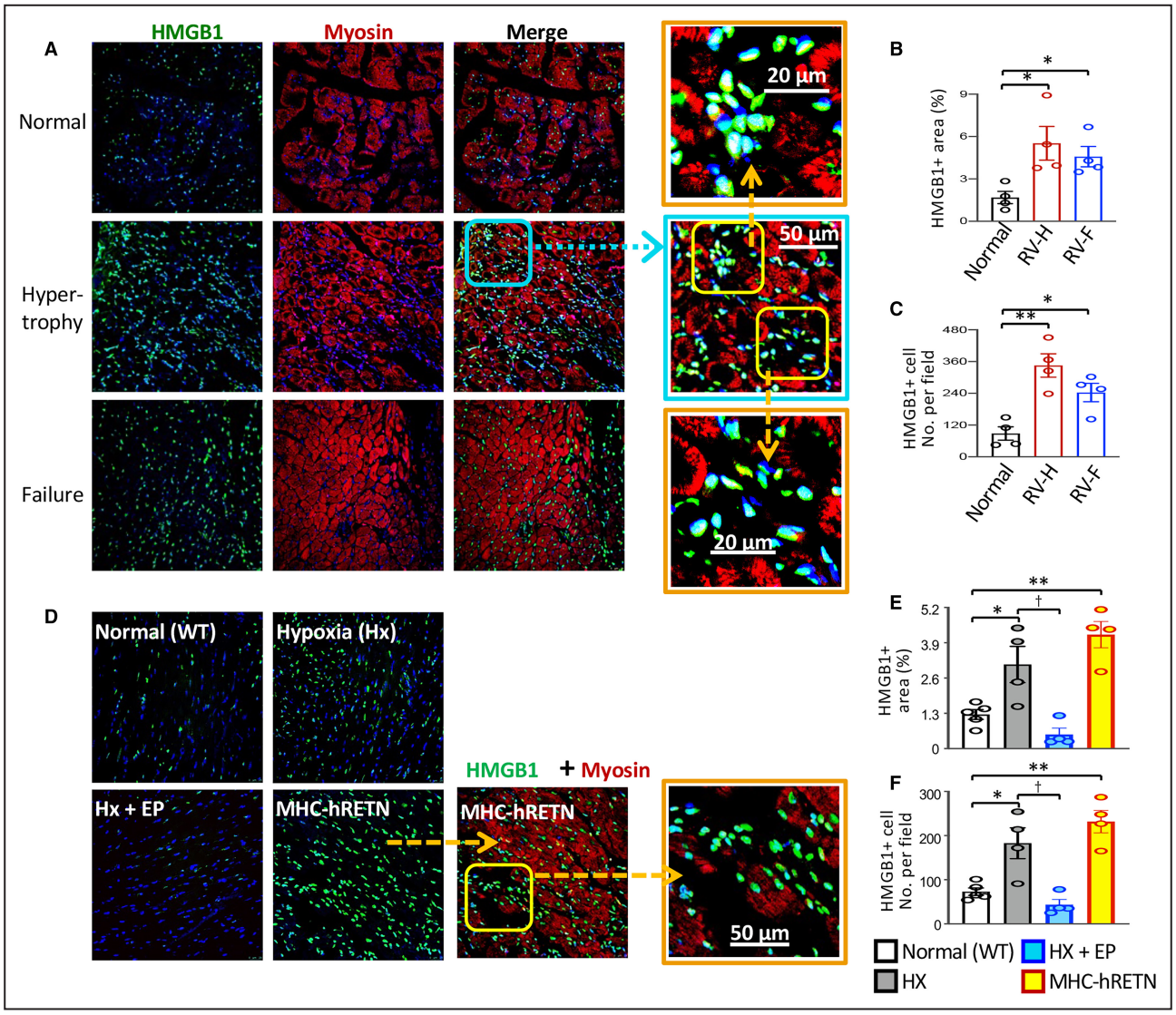

Figure 4. Hresistin activates HMGB1 signaling in the RV during RV r dysfunction.
A, Immunofluorescence images of hypertrophic RV (RV-H, 2 weeks post-MCT induction) and failing RV (RV-F, 4 weeks post-MCT induction) from MCT-treated rats. Sections were stained with anti-HMGB1 antibody (green), costained with anti-myosin (red), and counterstained with DAPI (blue). Representative photographs of 4 individual animals per group. Original magnification: ×200. Boxed region in the RV-H group is shown at higher magnification to the right (×400). Further magnification (×1000) of the 2 framed areas are shown in the upper and lower panels to illustrate the HMGB1-positive, myosin-negative cells that infiltrated the myocardial interstitium. **B** and **C**, Quantitative analysis of data in **A**. Percentage of area positive for HMGB1 signal (HMGB1+) in rat right heart determined with Adobe Photoshop software (**B**) and the number (No.) of HMGB1-positive cells counted (**C**) on 5 randomly chosen RV fields in each animal at 200-fold magnification. Data are presented as mean±SEM (n=4 animals per group). *P<0.05, **P<0.01 vs normal (non-MCT-treated) rats. **D**, Immunofluorescence images of RV tissue from wild-type (WT) mice on post-hypoxia day 4 and from MHC-hRETN humanized mice. Some hypoxic (Hx) mice received daily intraperitoneal injections of the HMGB1-specific inhibitor ethyl pyruvate (EP, 50 mg/kg) for 4 days. Representative photographs of 4 individual animals per group. Original magnification: ×200. In the MHC-hRETN group, the corresponding co-staining for HMGB1 (green) with myosin (red) is presented in the lower panel, and the boxed region in it is shown at higher magnification (×400) on the left. **E** and **F**, Quantitative analysis of data in **D**. Percentage of area positive for HMGB1 signal in mouse right hearts was determined (**E**), and HMGB1-positive cells (per observed field) were counted (**F**). Data are presented as mean±SEM (n=5 animals per group for the control [normal WT] group and n=4 animals per group for the other 3 groups [Hx, Hx+EP, and MHC-hRETN]; the dots in the graphs represent single individuals). *P<0.05, **P<0.01 (increase) vs normal WT mice; †P<0.05 (decrease) vs the hypoxia (Hx)-only group. DAPI indicates 4'6-diamidino-2-phenyl-indole; EP, ethyl pyruvate; HMGB1, high mobility group box 1; hRETN, human resistin; hx, hypoxia; MCT, monocrotaline; MHC, myosin heavy chain; RV-F, failing right ventricle; and RV-H, hypertrophic right ventricle.

myosin-negative cells infiltrated into the interstitium of the RV tissues, indicating that accumulating immune cells are also a source of HMGB1. This DAMP signal peaked in the hypertrophic myocardium (Figure 4A through 4C) and then declined slightly but remained elevated in the failing stage (Figure 4A through 4C).

We demonstrated that HMGB1-positive cell infiltration, also observed in the early onset of RVD (posthypoxic day-4, during the early PH inflammation phase)[12,14] (Figure 4D through 4F), was reversed by the specific HMGB1 inhibitor ethyl pyruvate (EP; Figure 4D through 4F). The upregulation of HMGB1 expression was even more striking in RV tissue that overexpressed Hresistin (Figure 4D through 4F).

Associated with HMGB1 elevation, we observed a marked increase in Ki67-positive cells in hypertrophic and failing RV tissue in the monocrotaline-induced rat PH model compared with that in the non-monocrotaline control rats (Figure 5A and 5B). The Ki67-positive cells were present during the early posthypoxia inflammatory phase (Figure 5C and 5D). Intriguingly, Hresistin knock-in induced a much stronger proliferation of Ki67-positive cells in RV tissues than did hypoxia exposure in wild-type mice (Figure 5C and 5D). These Hresistin-induced Ki67 signals were also observed in the interstitium of myosin-positive cardiomyocytes (Figure 5C) and had an expression pattern similar to that of HMGB1 (Figure 4D). Further colocalization analysis revealed that most of the Ki67- positive cells were the infiltrating leukocytes (F4/80+ macrophages and MPO+ neutrophils), and a few Ki67- positive cells were also the vimentin+ fibroblasts,[36] in the Hresistin-overexpressing RV tissues (Figure 5E), indicating the mechanism that Hresistin signaling induces RV remodeling through the inflammatory cytokine-associated cardiac fibrosis. The enhancement of this proliferative marker was reversed by administration of the HMGB1 antagonist EP (Figure 5C and 5D). Thus, Ki67 signal may mediate the effects of Hresistin/HMGB1 pathway axis to further amplify RV inflammation.

Collectively, these data suggest that Hresistin signaling triggers the HMGB1-dependent inflammatory response to initiate RVD. Moreover, it is a self-replenishing mechanism that sustains this proinflammatory state and continuously fuels RVD, thereby leading to RV remodeling and failure in chronic PH.

Anti-Hresistin Antibody Ameliorates RV Dysfunction and Remodeling in the Rat PH Models

To validate the pathogenetic role of Hresistin in RV dysfunction and remodeling, we developed a series of therapeutic antibodies against Hresistin and identified a lead antibody that binds both Hresistin[24] and rodent RELMα (Figure 6C). When administered in the chronic hypoxia-induced PH rat model, this antibody ameliorated RV wall thickness (Figure 6A) and improved RV function (Figure 6B). Blocking Hresistin/RELMα with the neutralizing antibody also significantly reduced RV systolic pressure (Figure 6D) and RV hypertrophy (Figure 6E) in this rat PH model. Moreover, in the monocrotaline-induced PH rat model, the anti-Hresistin therapeutic antibody prolonged survival of experimental animals in heart failure (Figure 6F). Mechanistically, in the RV tissues of these PH rats, hypoxia induced the production of RELMα, HMGB1, and the hypertrophic biomarkers atrial natriuretic peptide and β-MHC (Figure 7A and 7B). Consistently, in the cardiomyocytes isolated from neonatal rats, Hresistin overexpression mediated by adeno-associated virus transfection induced the expression of HMGB1, and β-MHC in vitro (Figure 7C and 7D). This was prevented by pretreatment with the anti-Hresistin/RELMα antibody (Figure 7C and 7D). In the neonatal rat cardiomyocytes, the Hresistin overexpression-induced hypertrophic proteins expression (atrial natriuretic peptide and β-MHC) (Figure 7E and 7F) and cell size increase (Figure 7G) were abrogated by pretreatment of the HMGB1 inhibitor EP, validating the role of HMGB1 in mediating the Hresistin-induced myocardial dysfunction in RV tissues during PH development. These findings suggest that our generated antibody against Hresistin/RELMα proteins has potential therapeutic value for human PH-associated RV dysfunction and failure.

DISCUSSION

We present a novel concept that Hresistin signaling is a causal factor for the cardiac dysfunction and remodeling (Figure 8) that parallels the Hresistin/RELMα-induced vascular remodeling in lungs during PH. This study directly links RELMs to RVD, highlighting their unique role in the immune interaction between lungs and the RV in PH. The humanized mouse model of cardiac-restricted Hresistin overexpression enabled us to explore the specific cardiac action of Hresistin signaling from a more translational and mechanistic perspective. Moreover, the newly developed anti-Hresistin antibody had beneficial effects against RVD and may hold promise for preventing or reversing RV failure in human disease.

The RV has distinguishing physiologic properties in response to pathologic insults,[37] but the mechanism underlying PH-associated RV dysfunction is still unclear. Based on our mechanistic data, we believe Hresistin triggers DAMP-associated inflammation that eventually leads to RV failure. The kinases PKA and AMPK govern Ca^{2+} channels, force-frequency response, and myofilament behavior in cardiomyocytes.[38–48] Dysregulation of these pathways could decrease cardiac contractility as we observed in the mouse Hresistin-overexpressing RV. These kinases have been implicated in inflammatory pathogenesis. PKA was involved in inflammasome activation in macrophages,[49,50] indicating a link to HMGB1 signaling, given the reported inflammasome-dependent release

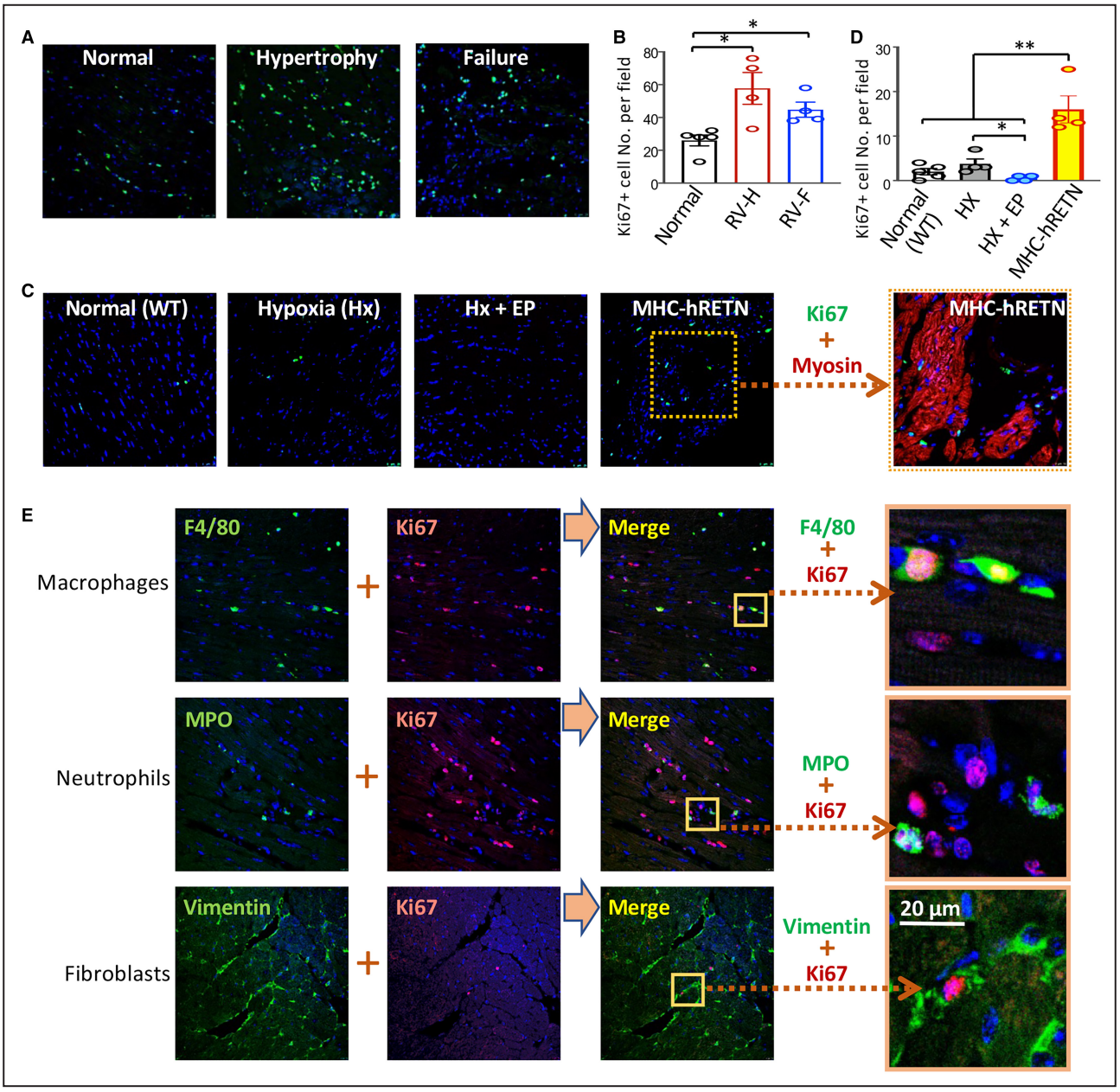

Figure 5. Hresistin/HMGB1 signaling axis upregulates Ki67 expression in RV.
A, Sections of RV tissues during hypertrophy or failure (as described in above panel A) were stained with anti-Ki67 antibody (green) and counterstained with DAPI (blue). Representative photographs of 4 individual animals per group. Magnification: ×200. **B**, Quantitative analysis of data from A. Ki67-positive (Ki67+) cells were counted on 5 randomly chosen fields of RV sections in each animal at ×200 magnification. Data are presented as mean±SEM (n=5 animals per group for the normal control group and n=4 animals per group for the groups of RV-H and RV-F; the dots in the graphs represent single individuals). *P<0.05 vs normal (non-MCT-treated) rats. **C**, Immunofluorescence images of RV tissue from WT mice exposed to 4 days of hypoxia with or without the HMGB1 inhibitor EP and from cardiac-specific MHC-hRETN-overexpressing mice. The boxed region in the fourth panel is shown at higher magnification (×400) on the right with costaining for Ki67 (green) and myosin (red). Representative photographs of 5 individual animals per group. Original magnification: ×200. **D**, Quantitative analysis of data in **C**. The Ki67-positive cells were counted (per observed field). Data are presented as mean±SEM (n=5 animals per group for the control [normal WT] group and n = 4 animals per group for the other 3 groups [Hx, Hx+EP, and MHC-hRETN]). *P<0.05, **P<0.01. **E**, In the RV tissues of the MHC-hRETN-overexpressing mice, Ki67 (red, middle panels) was further costained with the markers (green, left panels) of macrophages (F4/80), neutrophils (MPO), or fibroblasts (Vimentin). Images were merged in the right panels. The boxed areas were further enlarged in the far right panels showing the double positive cells. Representative photographs of 4 individual animals per group. Original magnification: ×400. DAPI indicates 4'6-diamidino-2-phenyl-indole; EP, ethyl pyruvate; HMGB1, high mobility group box 1; h-RETN, human resistin; Hx, hypoxia; MCT, monocrotaline; MHC, myosin heavy chain; MPO, myeloperoxidase; RV-F, failing right ventricle; RV-H, hypertrophic right ventricle; and WT, wild type.

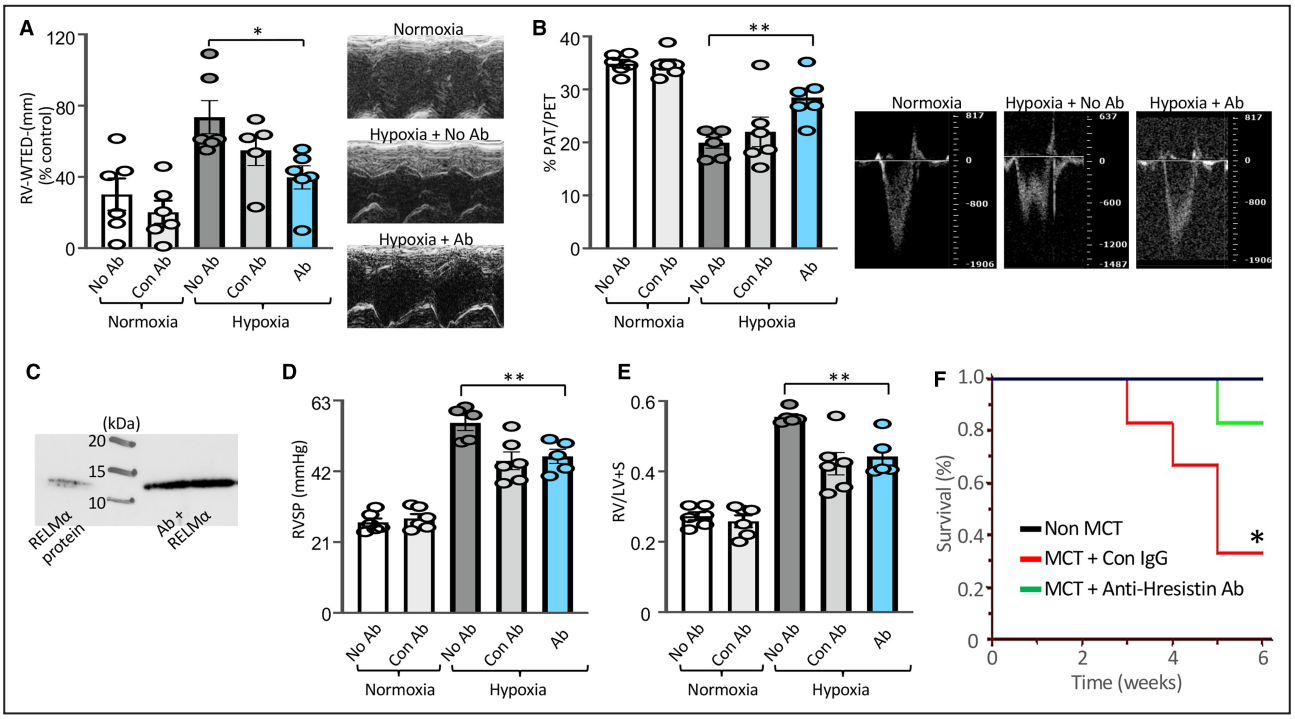

Figure 6. Anti-Hresistin human antibody ameliorates RV dysfunction in rats with PH.
The anti-Hresistin antibody (Ab) or the isotype-matched control IgG1 (Con IgG) at 4 mg/kg were administered intraperitoneally twice a week in the hypoxia-induced PH rats. **A** and **B**, Echocardiographic analysis of right ventricular (RV) wall thickness and pulmonary artery blood velocity in Ab-treated hypoxic rats. RV wall thickness external diameter (RV-WTED) was measured as the distance from the free wall to the interventricular septum (millimeter) in the parasternal long-axis view using M-mode (**A**). Data are expressed as a percentage of the value of normoxic control mice. The anti-Hresistin Ab treatment also lengthened pulmonary artery acceleration time (PAT). Results of pulsed wave Doppler measurement of PAT are shown in **B**. PAT values were normalized by pulmonary ejection time (PET). Data are expressed as means±SEM (n=6 animals per group). **P*<0.05, ***P*<0.01 vs hypoxia (no Ab) group. Representative echocardiographic images are shown in the right panels. **C**, Immunoprecipitation analysis of the binding of rat RELMα to the human therapeutic Ab targeting Hresistin. The protein-Ab binding was detected by western blotting with the anti-Hresistin antibody from R&D (AF1359). Recombinant rat RELMα protein was loaded as the positive control. **D** and **E**, Analysis of RV hypertrophy and hemodynamics in the hypoxia (Hx)-induced rat PH model. We measured the RV systolic pressure (RVSP) (**D**) and Fulton index (ratio of RV weight/LV+S weight) (**E**). Data are presented as means±SEM (normal no Ab: n=6, normal con Ab: n=6, hypoxia no Ab: n=5, hypoxia con Ab: n=6, hypoxia Ab: n=5; n refers to the number of animals per group). ***P*<0.01 vs Hx-treated group without Ab treatment. **F**, Results of treatment with the human antibody targeting Hresistin to improve the survival rate among rats with monocrotaline-induced PH. **P*<0.05 by log rank test; n=6 animals in each group. LV+S indicates left ventricle plus septum; MCT, monocrotaline; PH, pulmonary arterial hypertension; and RELMα, resistin-like molecule-α.

of HMGB1.[51–54] More notably, in humanized resistin mice with lipopolysaccharide-induced acute lung injury, Hresistin reduced AMPK and elevated HMGB1 in lungs,[35] consistent with our cardiac findings (Figures 3 and 4). These results suggest that HMGB1 is a key inflammatory element associated with RV dysfunction observed in Hresistin-induced RVD.

Inflammation is believed to be a mechanism that underlies RVD onset and progression.[55] Hresistin and its rodent homolog RELMα have been identified as TH2 inflammatory mediators in pulmonary diseases. Our recent studies in lungs showed that Hresistin/RELMα triggers HMGB1 signaling to mediate pulmonary vascular inflammation,[16,17] which is associated with the Hresistin/RELMα-induced recruitment of macrophages.[17] An alarmin, HMGB1, acts as an endogenous danger signal to regulate inflammatory response through an autocrine and paracrine manner by activating RAGE or TLR4.[56,57] Moreover, HMGB1 has been reported to have a critical role in inflammatory heart diseases.[58,59] Here, in our humanized mouse model, we observed activation of HMGB1 and the consequent ki67 in the RV. The proliferation of macrophages has been determined as a mechanism of RV failure in PH by studies on the monocrotaline-induced rat PH model.[60] In the current study, the Hresistin/HMGB1 signaling axis amplifies inflammation through enhancing the proliferation (Figure 5E) and recruitment of the immune cells in the RV and possibly expression in the myocyte itself. These findings suggest that Hresistin-triggered DAMP signaling not only ignites but also fuels the sterile inflammatory response during RVD onset and progression. Hresistin-initiated DAMP-dependent cardiac inflammation is likely an early response to injury

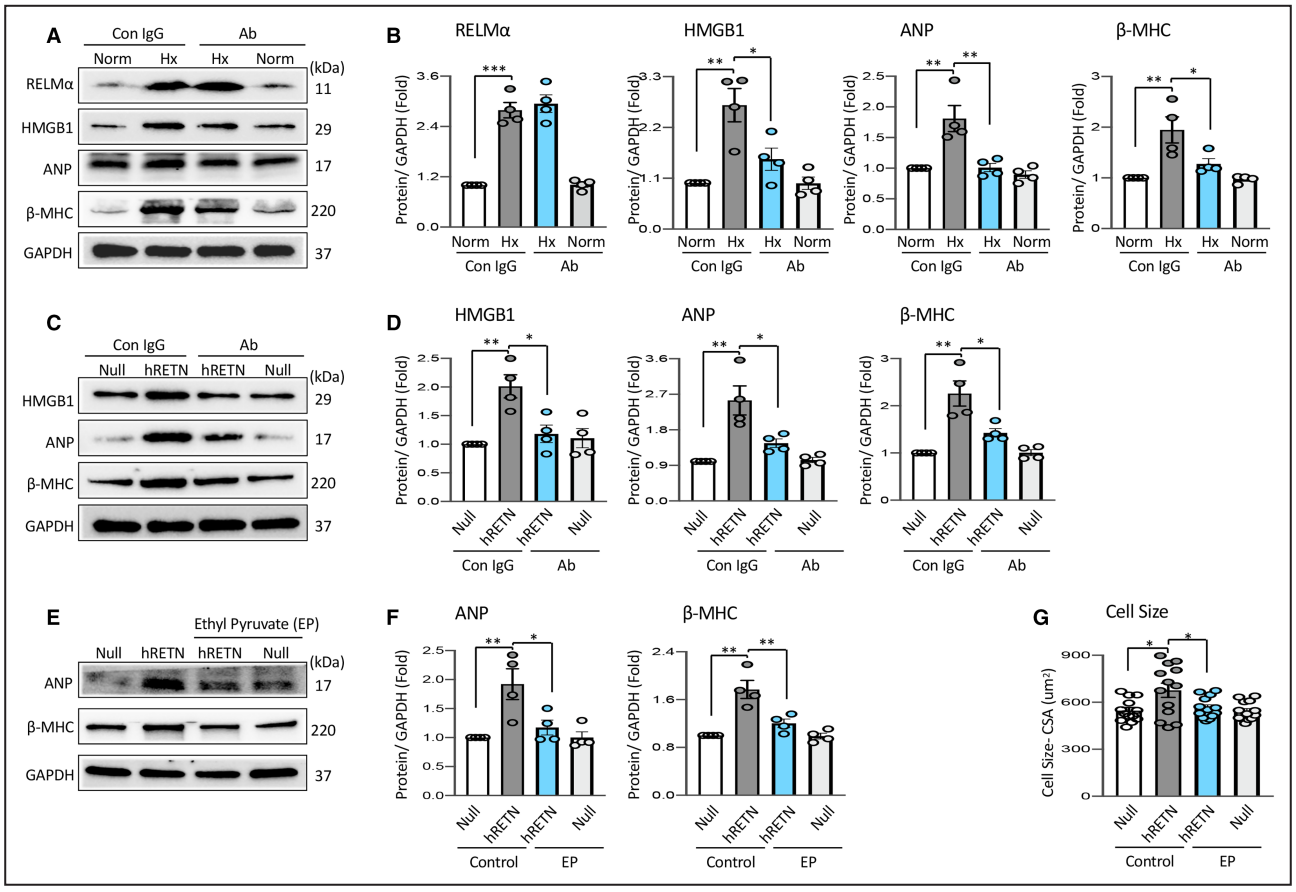

Figure 7. Hresistin/HMGB1 signaling axis induction of cardiac dysfunction and hypertrophy.
A, Representative immunoblots of the protein levels of RELMα, HMGB1, and the hypertrophy markers for atrial natriuretic peptide (ANP) and myosin heavy chain-β (β-MHC) in RV showing anti-Hresistin Ab inhibition of the hypoxia-induced expression of HMGB1 and RV hypertrophy markers in the RV of PH rats in vivo. **B**, Quantitative analysis of data in A. n=4 rats per group, one-way ANOVA with Tukey post hoc analysis for multiple group comparisons. **C**, Immunoblots showing anti-Hresistin Ab prevention of the Hresistin-induced expression of HMGB1 and RV hypertrophy markers in the neonatal rat cardiomyocytes (NRCMs) in vitro. The primary cultured NRVMs were pretreated with 3 μg/mL Con IgG or the anti-Hresistin Ab followed by transduction of MOI-300 GFP-tagged adeno-associated virus (AAV) expressing the Hresistin (hRETN). Empty AAV vector (null) served as the negative control. Representative immunoblots are shown (n=4 per group). **D**, Quantitative analysis of data in C. Data are expressed as means±SEM (n=4 per group). **P*<0.05, ***P*<0.01, ****P*<0.001. **E** through **G**, Representative and quantitative WB images and quantitative analysis of the HMGB1 inhibitor ethyl pyruvate (EP) attenuation of the Hresistin-induced cardiac hypertrophy in NRCMs in vitro. The primary NRVMs were pretreated with 5 μmol/L EP followed by MOI-300 AAV-hRETN transduction. Representative WB images (**E**) and quantitative analysis (**F**) of ANP and β-MHC protein are displayed (n=4 per group). Quantification of the cell surface area of NRCMs is shown in G (n=13 per group). **P*<0.05, ***P*<0.01. Ab indicates antibody; GFP, green fluorescent protein; HMGB1, high mobility group box 1; Hresistin, human resistin; Hx, hypoxia; NRVM, neonatal rat cardiomyocyte; PH, pulmonary arterial hypertension; RELMα, resistin-like molecule-α; RV, right ventricle; and WB, western blot.

that leads to subsequent metabolic disarrangement. Thus, inflammation, metabolic derangement, impaired cardiac function, and adverse structural remodeling may occur on a time continuum that is initiated by the metabolism-regulating activity of HMGB1.[61] Additional study is required to elucidate this mechanism.

The time course over which Hresistin/RELMα activates inflammation may also help shed light on the transition from adaptive remodeling to maladaptive RV failure in patients with PH. Inflammatory cells are more numerous in the RV of patients with SSc-associated PH than in that of patients with other types of PH. Additionally, the high number of inflammatory cells is associated with the morbidity of RV failure in these patients,[55,62] suggesting that inflammation contributes to development of RV failure. As a significant proportion of the WHO group-1 PH, the SSc-PH heralds a particularly poor prognosis compared with patients with subtypes of the group-1 PH including idiopathic PH, despite having similar measures of RV load.[63,64] Inflammation is a pathogenetic factor of cardiac involvement in SSc-PH.[63] Mechanistically, compared with idiopathic PH, SSc-PH exhibits depressed RV contractile reserve,[65] associated with reduced calcium

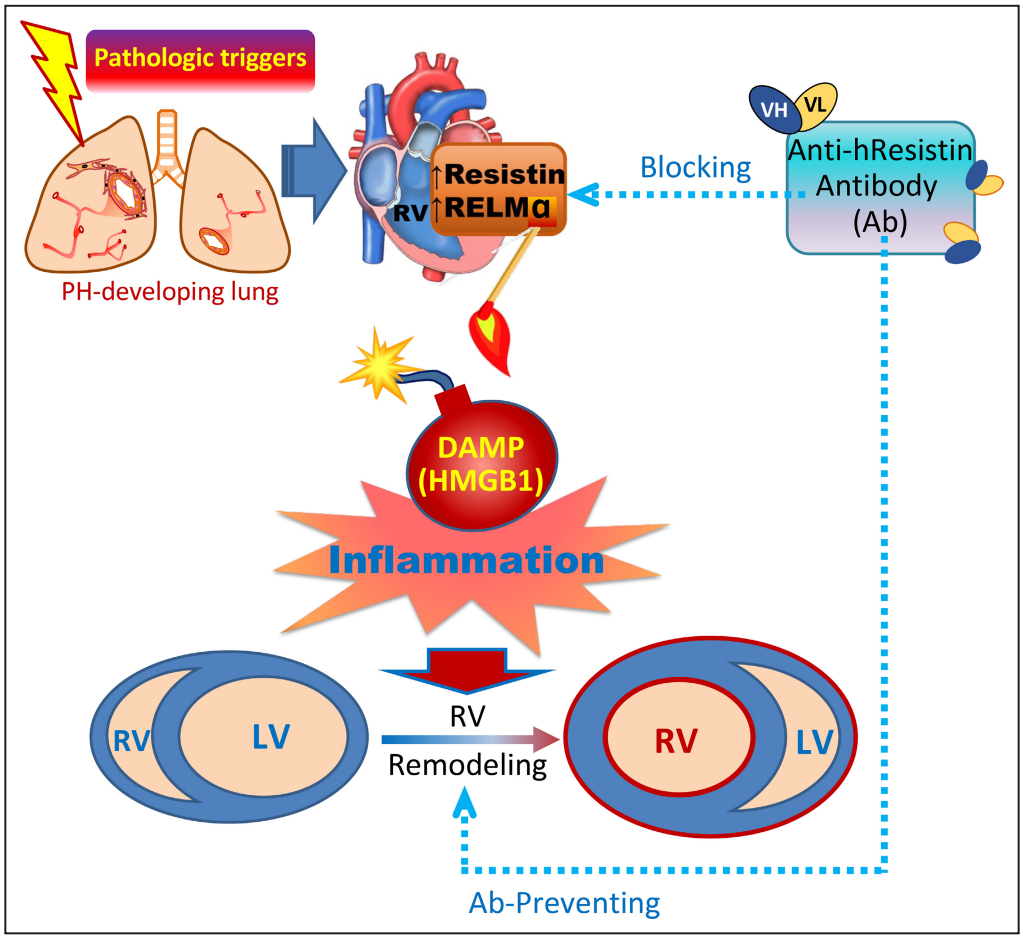

Figure 8. Schematic illustration of Hresistin-induced cardiac inflammation and dysfunction.
During pulmonary arterial hypertension (PH) development, Hresistin activates the damage-associated molecular pattern (DAMP), signaling triggering of inflammation in the right ventricle (RV) and contributing to RV dysfunction pathogenesis. Targeting the Hresistin signaling cascade may constitute a novel therapeutic approach to RV dysfunction and other related cardiac diseases in humans. HMGB1 indicates high mobility group box 1; Hresistin, human resistin; LV, left ventricle; and RELMα, resistin-like molecule-α.

recycling, which is caused by PKA suppression.[65,66] Given the amplified inflammation (Figure 4), fibrosis (Figure 3E), impaired contractility, decreased intracellular Ca^{2+} availability (Figure 3A), and the suppressed PKA (Figure 3B) in the Hresistin-overexpressing RV tissues, it suggests the activation of Hresistin signaling in the RV of SSc-PH (Figure 1B) as the pathogenetic mechanism of RV dysfunction, remodeling, and failure of this PH subform. Moreover, we have observed RELMα activation as a key pathogenetic mechanism in hypoxia- and monocrotaline-induced models of PAH and RV dysfunction,[1] suggesting Hresistin as a critical pro-inflammatory mediator of RV remodeling and failure in a broad array of human PAH diseases. Nevertheless, further studies are warranted on the role of Hresistin signals in RV pathology of other PAH subtypes. The role of inflammation in LV failure has been better studied,[67,68] but anti-inflammatory therapy for LV failure has failed so far.[55] In our study, Hresistin/RELMα activation in the RV during PH development, and Hresistin/RELMα-mediated accumulation of HMGB1- and Ki67-producing inflammatory cells, all peaked in the hypertrophied RV and declined in the failing RV (Figures 1, 4, and 5). These findings suggest that RELM-DAMP signaling may facilitate the early, intensified damage-triggered inflammatory response that leads to later pathologic remodeling. This response may be responsible for the RV's transition from a compensated to a decompensated state. Hresistin thereby could constitute a therapeutic target for preventing RV dysfunction and the subsequent progression to RV failure. This possibility is supported by the promising results of the therapeutic anti-Hresistin antibody, which ameliorated cardiac remodeling and prolonged survival of PH rats (Figures 6 and 7), given that survival in PH is closely related to RV function.[69]

One limitation of our work is that although we focused on the RV, the MHC-Hresistin humanized model

is not RV-specific. It is difficult or impossible to create an animal model with exclusive RV expression. To date there are no RV-specific markers to target the genetic expression specifically to the right heart. In addition, given that immunoregulation by Hresistin/RELMα leads to fibrosis in lungs,[70] and that we observed Hresistin-induced heart fibrosis in the humanized mice (Figure 3), future studies are warranted to explore the proinflammation-to-profibrotic phenotype switch in RELM-DAMP-activated immune cells and myocytes, and to test the antifibrotic properties of the anti-Hresistin antibody. Nevertheless, we were able to show that Hresistin activation triggers RV inflammation, metabolic derangement, and subsequent hypertrophy that leads to the initiation and progression of right ventricular failure in PH and that blocking Hresistin signaling with a human antibody may prevent or reverse the PH-associated RVD in humans.

ARTICLE INFORMATION

Revised January 3, 2023; accepted January 6, 2023.

Affiliations

Department of Anesthesiology and Critical Care Medicine, Johns Hopkins University School of MedicineBaltimore, MD (Q.L., S.K., U.K., X.Y., W.Y., J.T.S., W.D.G., R.A.J.); Department of Anesthesiology, Qilu Hospital, Cheeloo College of Medicine, Shandong UniversityJinan, China (X.Y.); and Department of Cardiovascular Medicine, Xiangya Hospital, Central South UniversityChangsha, China (W.Y.).

Acknowledgments

The authors thank Claire F. Levine, MS, ELS and the Johns Hopkins Editorial Assistance Services Initiative for support in editing this manuscript.

Sources of Funding

This work was supported by NIH Centers for Advanced Diagnostics and Experimental Therapeutics in Lung Diseases (CADET) I (P50HL107182), CADET II (5UH2HL123827–02) and R01HL138497 grants (to R.A.J.), American Heart Association (AHA) Grant-in-Aid 17GRNT33670387 (to W.D.G), and AHA grant #938614/2022 (to Q. L.).

Disclosures

None.

Supplemental Material

Figure S1

REFERENCES

1. Lin Q, Johns RA. Resistin family proteins in pulmonary diseases. *Am J Physiol Lung Cell Mol Physiol.* 2020;319:L422–L434. doi: 10.1152/ajplung.00040.2020
2. Jung YH, Ren X, Suffredini G, Dodd OJ, Gao WD. Right ventricular diastolic dysfunction and failure: a review. *Heart Fail Rev.* 2022;27:1077–1090. doi: 10.1007/s10741-021-10123-8
3. Angelini DJ, Su Q, Yamaji-Kegan K, Fan C, Skinner JT, Champion HC, Crow MT, Johns RA. Hypoxia-induced mitogenic factor (HIMF/FIZZ1/RELMα) induces the vascular and hemodynamic changes of pulmonary hypertension. *Am J Physiol Lung Cell Mol Physiol.* 2009;296:L582–L593. doi: 10.1152/ajplung.90526.2008
4. Su Q, Zhou Y, Johns RA. Bruton's tyrosine kinase (BTK) is a binding partner for hypoxia induced mitogenic factor (HIMF/FIZZ1) and mediates myeloid cell chemotaxis. *FASEB J.* 2007;21:1376–1382. doi: 10.1096/fj.06-6527com
5. Yamaji-Kegan K, Su Q, Angelini DJ, Champion HC, Johns RA. Hypoxia-induced mitogenic factor has proangiogenic and proinflammatory effects in the lung via VEGF and VEGF receptor-2. *Am J Physiol Lung Cell Mol Physiol.* 2006;291:L1159–L1168. doi: 10.1152/ajplung.00168.2006
6. Chemaly ER, Hadri L, Zhang S, Kim M, Kohlbrenner E, Sheng J, Liang L, Chen J, K-Raman P, Hajjar RJ, et al. Long-term in vivo resistin overexpression induces myocardial dysfunction and remodeling in rats. *J Mol Cell Cardiol.* 2011;51:144–155. doi: 10.1016/j.yjmcc.2011.04.006
7. Holcomb IN, Kabakoff RC, Chan B, Baker TW, Gurney A, Henzel W, Nelson C, Lowman HB, Wright BD, Skelton NJ, et al. FIZZ1, a novel cysteine-rich secreted protein associated with pulmonary inflammation, defines a new gene family. *EMBO J.* 2000;19:4046–4055. doi: 10.1093/emboj/19.15.4046
8. Teng X, Li D, Champion HC, Johns RA. FIZZ1/RELMα, a novel hypoxia-induced mitogenic factor in lung with vasoconstrictive and angiogenic properties. *Circ Res.* 2003;92:1065–1067. doi: 10.1161/01.RES.0000073999.07698.33
9. Angelini DJ, Su Q, Kolosova IA, Fan C, Skinner JT, Yamaji-Kegan K, Collector M, Sharkis SJ, Johns RA. Hypoxia-induced mitogenic factor (HIMF/FIZZ1/RELMα) recruits bone marrow-derived cells to the murine pulmonary vasculature. *PLoS One.* 2010;5:e11251. doi: 10.1371/journal.pone.0011251
10. Angelini DJ, Su Q, Yamaji-Kegan K, Fan C, Skinner JT, Poloczek A, El-Haddad H, Cheadle C, Johns RA. Hypoxia-induced mitogenic factor (HIMF/FIZZ1/RELMα) in chronic hypoxia- and antigen-mediated pulmonary vascular remodeling. *Respir Res.* 2013;14:1. doi: 10.1186/1465-9921-14-1
11. Johns RA. Th2 inflammation, hypoxia-induced mitogenic factor/FIZZ1, and pulmonary hypertension and vascular remodeling in schistosomiasis. *Am J Respir Crit Care Med.* 2010;181:203–205. doi: 10.1164/rccm.200912-1827ED
12. Johns RA, Takimoto E, Meuchel LW, Elsaigh E, Zhang A, Heller NM, Semenza GL, Yamaji-Kegan K. Hypoxia-inducible factor 1alpha is a critical downstream mediator for hypoxia-induced mitogenic factor (FIZZ1/RELMα)-induced pulmonary hypertension. *Arterioscler Thromb Vasc Biol.* 2016;36:134–144. doi: 10.1161/ATVBAHA.115.306710
13. Yamaji-Kegan K, Su Q, Angelini DJ, Myers AC, Cheadle C, Johns RA. Hypoxia-induced mitogenic factor (HIMF/FIZZ1/RELMa) increases lung inflammation and activates pulmonary microvascular endothelial cells via an IL-4-dependent mechanism. *J Immunol.* 2010;185:5539–5548. doi: 10.4049/jimmunol.0904021
14. Yamaji-Kegan K, Takimoto E, Zhang A, Weiner NC, Meuchel LW, Berger AE, Cheadle C, Johns RA. Hypoxia-induced mitogenic factor (FIZZ1/RELMa) induces endothelial cell apoptosis and subsequent interleukin-4-dependent pulmonary hypertension. *Am J Physiol Lung Cell Mol Physiol.* 2014;306:L1090–L1103. doi: 10.1152/ajplung.00279.2013
15. Fan C, Fu Z, Su Q, Angelini DJ, Van Eyk J, Johns RA. S100a11 mediates hypoxia-induced mitogenic factor (HIMF)-induced smooth muscle cell migration, vesicular exocytosis, and nuclear activation. *Mol Cell Proteomics.* 2011;10(M110):000901. doi: 10.1074/mcp.M110.000901
16. Lin Q, Fan C, Gomez-Arroyo J, Van Raemdonck K, Meuchel LW, Skinner JT, Everett AD, Fang X, Macdonald AA, Yamaji-Kegan K, et al. HIMF (hypoxia-induced mitogenic factor) signaling mediates the HMGB1 (high mobility group box 1)-dependent endothelial and smooth muscle cell crosstalk in pulmonary hypertension. *Arterioscler Thromb Vasc Biol.* 2019;39:2505–2519. doi: 10.1161/ATVBAHA.119.312907
17. Lin Q, Fan C, Skinner JT, Hunter EN, Macdonald AA, Illei PB, Yamaji-Kegan K, Johns RA. RELMα licenses macrophages for damage-associated molecular pattern activation to instigate pulmonary vascular remodeling. *J Immunol.* 2019;203:2862–2871. doi: 10.4049/jimmunol.1900535
18. Angelini DJ, Su Q, Yamaji-Kegan K, Fan C, Teng X, Hassoun PM, Yang SC, Champion HC, Tuder RM, Johns RA. Resistin-like molecule-b in scleroderma-associated pulmonary hypertension. *Am J Respir Cell Mol Biol.* 2009;41:553–561. doi: 10.1165/rcmb.2008-0271OC
19. Lewandoski M. Conditional control of gene expression in the mouse. *Nat Rev Genet.* 2001;2:743–755. doi: 10.1038/35093537
20. Yu Z, Redfern CS, Fishman GI. Conditional transgene expression in the heart. *Circ Res.* 1996;79:691–697. doi: 10.1161/01.RES.79.4.691
21. Zhu Z, Homer RJ, Wang Z, Chen Q, Geba GP, Wang J, Zhang Y, Elias JA. Pulmonary expression of interleukin-13 causes inflammation, mucus hypersecretion, subepithelial fibrosis, physiologic abnormalities, and eotaxin production. *J Clin Invest.* 1999;103:779–788. doi: 10.1172/JCI5909

22. Ren X, Schmidt W, Huang Y, Lu H, Liu W, Bu W, Eckenhoff R, Cammarato A, Gao WD. Fropofol decreases force development in cardiac muscle. *FASEB J.* 2018;32:4203–4213. doi: 10.1096/fj.201701442R
23. Huang Y, Lu H, Ren X, Li F, Bu W, Liu W, Dailey WP, Saeki H, Gabrielson K, Abraham R, et al. Fropofol prevents disease progression in mice with hypertrophic cardiomyopathy. *Cardiovasc Res.* 2020;116:1175–1185. doi: 10.1093/cvr/cvz218
24. Lin Q, Fan C, Skinner JT, Bejia D, Van Raemdonck K, Nakahara M, Yamaji-Kegan K, Johns RA Therapeutic effects of the generated antibodies targeting human resistin in pulmonary hypertension. *ATS (American Thoracic Society) Int Conf.* 2018;197:A7398.
25. Meng T, Ren X, Chen X, Yu J, Agrimi J, Paolocci N, Gao WD. Anesthetic agents isoflurane and propofol decrease maximal ca(2+)-activated force and thus contractility in the failing myocardium. *J Pharmacol Exp Ther.* 2019;371:615–623. doi: 10.1124/jpet.119.259556
26. Guihaire J, Deuse T, Wang D, Fadel E, Reichenspurner H, Schrepfer S. Sex differences in immunology: more severe development of experimental pulmonary hypertension in male rats exposed to vascular endothelial growth factor receptor blockade. *Biomed Res Int.* 2015;2015:1–7. doi: 10.1155/2015/765292
27. Tofovic SP. Estrogens and development of pulmonary hypertension: interaction of estradiol metabolism and pulmonary vascular disease. *J Cardiovasc Pharmacol.* 2010;56:696–708. doi: 10.1097/FJC.0b013e3181f9ea8d
28. Rafikov R, Nair V, Sinari S, Babu H, Sullivan JC, Yuan JX, Desai AA, Rafikova O. Gender difference in damage-mediated signaling contributes to pulmonary arterial hypertension. *Antioxid Redox Signal.* 2019;31:917–932. doi: 10.1089/ars.2018.7664
29. Provencher S, Archer SL, Ramirez FD, Hibbert B, Paulin R, Boucherat O, Lacasse Y, Bonnet S. Standards and methodological rigor in pulmonary arterial hypertension preclinical and translational research. *Circ Res.* 2018;122:1021–1032. doi: 10.1161/CIRCRESAHA.117.312579
30. Humbert M, Guignabert C, Bonnet S, Dorfmuller P, Klinger JR, Nicolls MR, Olschewski AJ, Pullamsetti SS, Schermuly RT, Stenmark KR, et al. Pathology and pathobiology of pulmonary hypertension: state of the art and research perspectives. *Eur Respir J.* 2019;53:1801887. doi: 10.1183/13993003.01887-2018
31. Boucherat O, Agrawal V, Lawrie A, Bonnet S. The latest in animal models of pulmonary hypertension and right ventricular failure. *Circ Res.* 2022;130:1466–1486. doi: 10.1161/CIRCRESAHA.121.319971
32. Shimauchi T, Boucherat O, Yokokawa T, Grobs Y, Wu W, Orcholski M, Martineau S, Omura J, Tremblay E, Shimauchi K, et al. PARP1-PKM2 axis mediates right ventricular failure associated with pulmonary arterial hypertension. *JACC Basic Transl Sci.* 2022;7:384–403. doi: 10.1016/j.jacbts.2022.01.005
33. Omura J, Habbout K, Shimauchi T, Wu WH, Breuils-Bonnet S, Tremblay E, Martineau S, Nadeau V, Gagnon K, Mazoyer F, et al. Identification of long noncoding rna H19 as a new biomarker and therapeutic target in right ventricular failure in pulmonary arterial hypertension. *Circulation.* 2020;142:1464–1484. doi: 10.1161/CIRCULATIONAHA.120.047626
34. Tao B, Kumar S, Gomez-Arroyo J, Fan C, Zhang A, Skinner J, Hunter E, Yamaji-Kegan K, Samad I, Hillel AT, et al. Resistin-like molecule α dysregulates cardiac bioenergetics in neonatal rat cardiomyocytes. *Front Cardiovasc Med.* 2021;8:574708. doi: 10.3389/fcvm.2021.574708
35. Jiang S, Park DW, Tadie JM, Gregoire M, Deshane J, Pittet JF, Abraham E, Zmijewski JW. Human resistin promotes neutrophil proinflammatory activation and neutrophil extracellular trap formation and increases severity of acute lung injury. *J Immunol.* 2014;192:4795–4803. doi: 10.4049/jimmunol.1302764
36. Tian L, Wu D, Dasgupta A, Chen KH, Mewburn J, Potus F, Lima PDA, Hong Z, Zhao YY, Hindmarch CCT, et al. Epigenetic metabolic reprogramming of right ventricular fibroblasts in pulmonary arterial hypertension: a pyruvate dehydrogenase kinase-dependent shift in mitochondrial metabolism promotes right ventricular fibrosis. *Circ Res.* 2020;126:1723–1745. doi: 10.1161/CIRCRESAHA.120.316443
37. Walker LA, Buttrick PM. The right ventricle: biologic insights and response to disease: updated. *Curr Cardiol Rev.* 2013;9:73–81. doi: 10.2174/157340313805076296
38. Shen X, Tan Z, Zhong X, Tian Y, Wang X, Yu B, Ramirez-Correa G, Murphy A, Gabrielson K, Paolocci N, et al. Endocardial endothelium is a key determinant of force-frequency relationship in rat ventricular myocardium. *J Appl Physiol.* 1985;2013(115):383–393. doi: 10.1152/japplphysiol.01415.2012
39. Muslin AJ, DeBosch B. Role of Akt in cardiac growth and metabolism. *Novartis Found Symp.* 2006;274:118–126; discussion 126–131, 152–115, 272–116
40. Varga ZV, Pipicz M, Baan JA, Baranyai T, Koncsos G, Leszek P, Kusmierczyk M, Sanchez-Cabo F, Garcia-Pavia P, Brenner GJ, et al. Alternative splicing of NOX4 in the failing human heart. *Front Physiol.* 2017;8:935. doi: 10.3389/fphys.2017.00935
41. Oliveira SM, Zhang YH, Solis RS, Isackson H, Bellahcene M, Yavari A, Pinter K, Davies JK, Ge Y, Ashrafian H, et al. AMP-activated protein kinase phosphorylates cardiac troponin I and alters contractility of murine ventricular myocytes. *Circ Res.* 2012;110:1192–1201. doi: 10.1161/CIRCRESAHA.111.259952
42. Ago T, Kuroda J, Pain J, Fu C, Li H, Sadoshima J. Upregulation of Nox4 by hypertrophic stimuli promotes apoptosis and mitochondrial dysfunction in cardiac myocytes. *Circ Res.* 2010;106:1253–1264. doi: 10.1161/CIRCRESAHA.109.213116
43. Kuroda J, Ago T, Matsushima S, Zhai P, Schneider MD, Sadoshima J. NADPH oxidase 4 (Nox4) is a major source of oxidative stress in the failing heart. *Proc Natl Acad Sci USA.* 2010;107:15565–15570. doi: 10.1073/pnas.1002178107
44. Ebert A, Joshi AU, Andorf S, Dai Y, Sampathkumar S, Chen H, Li Y, Garg P, Toischer K, Hasenfuss G, et al. Proteasome-dependent regulation of distinct metabolic states during long-term culture of human iPSC-derived cardiomyocytes. *Circ Res.* 2019;125:90–103. doi: 10.1161/CIRCRESAHA.118.313973
45. Steinhorn B, Sartoretto JL, Sorrentino A, Romero N, Kalwa H, Abel ED, Michel T. Insulin-dependent metabolic and inotropic responses in the heart are modulated by hydrogen peroxide from NADPH-oxidase isoforms NOX2 and NOX4. *Free Radic Biol Med.* 2017;113:16–25. doi: 10.1016/j.freeradbiomed.2017.09.006
46. Rockman HA, Koch WJ, Lefkowitz RJ. Seven-transmembrane-spanning receptors and heart function. *Nature.* 2002;415:206–212. doi: 10.1038/415206a
47. Harada M, Tadevosyan A, Qi X, Xiao J, Liu T, Voigt N, Karck M, Kamler M, Kodama I, Murohara T, et al. Atrial fibrillation activates AMP-dependent protein kinase and its regulation of cellular calcium handling: potential role in metabolic adaptation and prevention of progression. *J Am Coll Cardiol.* 2015;66:47–58. doi: 10.1016/j.jacc.2015.04.056
48. Ghigo A, Laffargue M, Li M, Hirsch E. PI3K and calcium signaling in cardiovascular disease. *Circ Res.* 2017;121:282–292. doi: 10.1161/CIRCRESAHA.117.310183
49. Moon JS, Nakahira K, Chung KP, DeNicola GM, Koo MJ, Pabon MA, Rooney KT, Yoon JH, Ryter SW, Stout-Delgado H, et al. NOX4-dependent fatty acid oxidation promotes NLRP3 inflammasome activation in macrophages. *Nat Med.* 2016;22:1002–1012. doi: 10.1038/nm.4153
50. Mortimer L, Moreau F, MacDonald JA, Chadee K. NLRP3 inflammasome inhibition is disrupted in a group of auto-inflammatory disease CAPS mutations. *Nat Immunol.* 2016;17:1176–1186. doi: 10.1038/ni.3538
51. Lamkanfi M, Sarkar A, Vande Walle L, Vitari AC, Amer AO, Wewers MD, Tracey KJ, Kanneganti TD, Dixit VM. Inflammasome-dependent release of the alarmin HMGB1 in endotoxemia. *J Immunol.* 2010;185:4385–4392. doi: 10.4049/jimmunol.1000803
52. Jia C, Zhang J, Chen H, Zhuge Y, Chen H, Qian F, Zhou K, Niu C, Wang F, Qiu H, et al. Endothelial cell pyroptosis plays an important role in Kawasaki disease via HMGB1/RAGE/cathespin B signaling pathway and NLRP3 inflammasome activation. *Cell Death Dis.* 2019;10:778. doi: 10.1038/s41419-019-2021-3
53. Yu S, Wang D, Huang L, Zhang Y, Luo R, Adah D, Tang Y, Zhao K, Lu B. The complement receptor C5aR2 promotes protein kinase R expression and contributes to NLRP3 inflammasome activation and HMGB1 release from macrophages. *J Biol Chem.* 2019;294:8384–8394. doi: 10.1074/jbc.RA118.006508
54. Vande Walle L, Kanneganti TD, Lamkanfi M. HMGB1 release by inflammasomes. *Virulence.* 2011;2:162–165. doi: 10.4161/viru.2.2.15480
55. Ren X, Johns RA, Gao WD. EXPRESS: right heart in pulmonary hypertension: from adaptation to failure. *Pulm Circ.* 2019;9:2045894019845611. doi: 10.1177/2045894019845611
56. van Beijnum JR, Buurman WA, Griffioen AW. Convergence and amplification of toll-like receptor (TLR) and receptor for advanced glycation end products (RAGE) signaling pathways via high mobility group B1 (HMGB1). *Angiogenesis.* 2008;11:91–99. doi: 10.1007/s10456-008-9093-5

57. Lin Q, Yang XP, Fang D, Ren X, Zhou H, Fang J, Liu X, Zhou S, Wen F, Yao X, et al. High-mobility group box-1 mediates toll-like receptor 4-dependent angiogenesis. *Arterioscler Thromb Vasc Biol.* 2011;31:1024–1032. doi: 10.1161/ATVBAHA.111.224048
58. Volz HC, Seidel C, Laohachewin D, Kaya Z, Muller OJ, Pleger ST, Lasitschka F, Bianchi ME, Remppis A, Bierhaus A, et al. HMGB1: the missing link between diabetes mellitus and heart failure. *Basic Res Cardiol.* 2010;105:805–820. doi: 10.1007/s00395-010-0114-3
59. Bangert A, Andrassy M, Muller AM, Bockstahler M, Fischer A, Volz CH, Leib C, Goser S, Korkmaz-Icoz S, Zittrich S, et al. Critical role of RAGE and HMGB1 in inflammatory heart disease. *Proc Natl Acad Sci USA.* 2016;113:E155–E164. doi: 10.1073/pnas.1522288113
60. Al-Qazazi R, Lima PDA, Prisco SZ, Potus F, Dasgupta A, Chen KH, Tian L, Bentley RET, Mewburn J, Martin AY, et al. Macrophage-NLRP3 activation promotes right ventricle failure in pulmonary arterial hypertension. *Am J Respir Crit Care Med.* 2022;206:608–624. doi: 10.1164/rccm.202110-2274OC
61. Jin K, Ma Y, Manrique-Caballero CL, Li H, Emlet DR, Li S, Baty CJ, Wen X, Kim-Campbell N, Frank A, et al. Activation of AMP-activated protein kinase during sepsis/inflammation improves survival by preserving cellular metabolic fitness. *FASEB J.* 2020;34:7036–7057. doi: 10.1096/fj.201901900R
62. Overbeek MJ, Mouchaers KT, Niessen HM, Hadi AM, Kupreishvili K, Boonstra A, Voskuyl AE, Belien JA, Smit EF, Dijkmans BC, et al. Characteristics of interstitial fibrosis and inflammatory cell infiltration in right ventricles of systemic sclerosis-associated pulmonary arterial hypertension. *Int J Rheumatol.* 2010;2010:1–10, DOI: 10.1155/2010/604615
63. Hassoun PM. The right ventricle in scleroderma (2013 Grover conference series). *Pulm Circ.* 2015;5:3–14. doi: 10.1086/679607
64. Kelemen BW, Mathai SC, Tedford RJ, Damico RL, Corona-Villalobos C, Kolb TM, Chaisson NF, Harris TH, Zimmerman SL, Kamel IR, et al. Right ventricular remodeling in idiopathic and scleroderma-associated pulmonary arterial hypertension: two distinct phenotypes. *Pulm Circ.* 2015;5:327–334. doi: 10.1086/680356
65. Hsu S, Houston BA, Tampakakis E, Bacher AC, Rhodes PS, Mathai SC, Damico RL, Kolb TM, Hummers LK, Shah AA, et al. Right ventricular functional reserve in pulmonary arterial hypertension. *Circulation.* 2016;133:2413–2422. doi: 10.1161/CIRCULATIONAHA.116.022082
66. Hsu S, Kokkonen-Simon KM, Kirk JA, Kolb TM, Damico RL, Mathai SC, Mukherjee M, Shah AA, Wigley FM, Margulies KB, et al. Right ventricular myofilament functional differences in humans with systemic sclerosis-associated versus idiopathic pulmonary arterial hypertension. *Circulation.* 2018;137:2360–2370. doi: 10.1161/CIRCULATIONAHA.117.033147
67. Cocco G, Jerie P, Amiet P, Pandolfi S. Inflammation in heart failure: known knowns and unknown unknowns. *Expert Opin Pharmacother.* 2017;18:1225–1233. doi: 10.1080/14656566.2017.1351948
68. Dick SA, Epelman S. Chronic heart failure and inflammation: what do we really know? *Circ Res.* 2016;119:159–176. doi: 10.1161/CIRCRESAHA.116.308030
69. Haddad F, Doyle R, Murphy DJ, Hunt SA. Right ventricular function in cardiovascular disease, part II: pathophysiology, clinical importance, and management of right ventricular failure. *Circulation.* 2008;117:1717–1731. doi: 10.1161/CIRCULATIONAHA.107.653584
70. Liu T, Yu H, Ullenbruch M, Jin H, Ito T, Wu Z, Liu J, Phan SH. The in vivo fibrotic role of FIZZ1 in pulmonary fibrosis. *PLoS One.* 2014;9:e88362. doi: 10.1371/journal.pone.0088362

SUPPLEMENTAL MATERIAL

Figure S1. Monocrotaline (MCT)-induced pulmonary hypertension causes right ventricular hypertrophy (RV-H) and failure (RV-F) in rats.

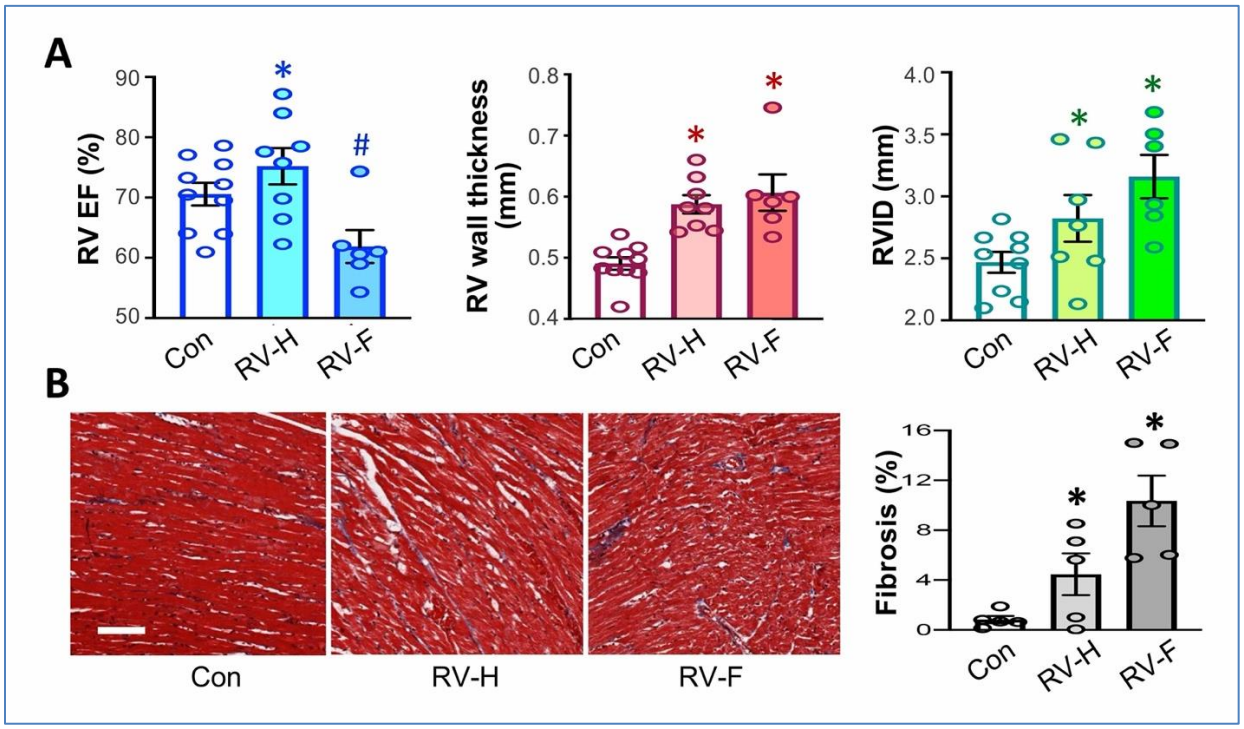

A, RV ejection fraction (EF), wall thickness and chamber diameter during development of RV-H and RV-F. We designated RV-H as compensated right ventricular hypertrophy with maintained RV EF (i.e. between 2.5-3.5 weeks after MCT injection), and RV-F as decompensated RV failure (i.e. after 4.5 weeks MCT injection when RV EF was significantly reduced). In EF test, control (Con, normal): n = 10, RV-H: n = 8, RV-F: n = 6. In RV wall thickness test, Con: n = 10, RV-H: n = 8, RV-F: n = 6. In RV chamber diameter (RVID) test, Con: n = 9, RV-H: n = 7, RV-F: n = 6. The n refers to the number of animals per group; the dots in the graphs represent single individuals. *,#$p < 0.05$ vs. 0 week (control). **B,** Masson staining of RVs of control, hypertrophied, and failed hearts (*left panels*) and quantification of fibrosis (*right panel*, data are means ± SEM, n = 5 animals per group, *$p < 0.05$ vs. control). Bar = 100 µm.